IJAME
Int. J. of Applied Mechanics and Engineering, 2024, vol.29, No.3, pp.47-68
DOI: 10.59441/ijame/189684

NUMERICAL STUDY OF ADAPTIVE GRIDS FOR LAMINAR FLOW IN A SUDDENLY EXPANDING CHANNEL

B.Kholboev[1*], M.Madaliev[2], A.Mirzoev[3], D.Asrakulova[1] and N.Engalicheva[1]
[1]Information System and Mathematical Sciences, Plekhanov Russian University of Economics, UZBEKISTAN,
[2]Fergana Polytechnic Institute, UZBEKISTAN
[3]Institute of Mechanics and Seismic Stability of Structures named after M.T.Urazbaev Academy of Sciences of the Republic of Uzbekistan, UZBEKISTAN
*E-mail: bakhodir.kholboev@gmail.com

In this article, a numerical study was carried out to study the dynamic adaptive grid method, based on the concept of the equidistribution method. The article explores a method for adapting the computational grid to solving two-dimensional Navier-Stokes differential equations, which describe the physical processes of gas dynamics specifically for the problem of a two-dimensional channel with an expansion coefficient (H/h) = *2*. Different flow characteristics were calculated at different Reynolds numbers Re = from *100* to *1000*, to get the actual thread behavior. Calculations are performed for laminar flow mode. The results of the longitudinal velocity profiles in different sections of the channel and the length of the primary and secondary vortices are obtained with a change in the Reynolds number after the ledge. For the numerical solution of this problem, a second-order accuracy McCormack scheme was used. To confirm the adequacy and reliability of the numerical results, a careful comparison was made with the experimental data of Armaly V.F. *et al.*, taken from the literature. It is also shown that as a result of using this method of adaptive grids, it is possible to improve the numerical accuracy obtained for a given number of node points. It is shown that the existing method of multiple 2D adaptive meshes makes it easier to concentrate meshes in the required areas. This method should prove useful for many Navier-Stokes flow calculations.

Key words: Navier-Stokes equations, dynamic adaptive grid, separated flow, control volume method, flat channel with reverse ledge.

1. Introduction

Nowadays, the study of separated flows is a classic problem in the field of fundamental fluid mechanics. This type of flow is a key object of study for understanding the phenomena of flow separation and reattachment, as well as the formation of recirculation zones. Flow separation processes have a wide range of applications in a variety of engineering applications, including the fluid dynamics of water around hydrofoils, air flow around compressor and turbine blades, and in piping and combustion chambers with abrupt cross-sectional changes. The study of hydrodynamic processes in rapidly expanding channels is an important aspect for understanding flow instabilities. Such flows arise in various technical systems and structures where there is a sharp change in the geometry of the channel (pipe) or the sudden appearance of obstacles, which can lead to a rupture or tangential withdrawal of the flow and a change in its kinematic structure. Particularly difficult are the conditions in a flat channel with a sharp expansion, where reverse vortices and complex separated flows arise in the zone behind the step, presenting significant difficulties for theoretical analysis and numerical modeling.

These problems pose the greatest challenge to verification because the flow structure is highly elliptical and is ideal for evaluating the performance of any numerical procedure. Initially, the flow has a straight entrance length, at which it can be either fully developed or undeveloped. Then a sharp expansion of the flow occurs, resulting in the formation of a large vortex. In this region, the flow structure is completely elliptical.

* To whom correspondence should be addressed

Then the flow restores its regime and becomes parabolic again. Typically, at low Reynolds numbers, reattachment increases, and as the flow enters transition, the recirculation zone shrinks, but then increases again as the flow velocity increases.

In 1910, Blasius [1] analytically studied the laminar separation of stationary two-dimensional flows of an incompressible fluid in straight channels. Subsequently, such problems were considered by many scientists to study the mechanisms of flow separation when observing and experimenting with differential schemes for solving the Navier-Stokes equations. Due to their considerable practical significance, existing flows have been theoretically and experimentally studied also for laminar [2-4] and turbulent [5-7] modes of motion of incompressible and compressible fluid. Most studies in this direction focus on flows in channels with bilateral symmetrical sharp expansion. [8-14]. The experimental data studied for this purpose in a flat channel were obtained in [8, 9], in which the formation of a circulation zone behind the bar was observed. A number of experimental scientists used equations of motion to calculate currents with a sharp expansion when approaching the edge layer [14, 15].

A significant, important body of work on dramatically expanding channels has been done by Armali *et al.* [4]. They performed and carried out a thorough analysis of the behavior of flows inside a backward-facing stepped channel experimentally and numerically [16-18]. A considerable amount of work was carried out by numerous people. Lee and Smith [19] used potential flow theory to derive the result of this problem. But potential flow theory could not predict the area of flow distribution or attachment behind the wall. Initial numerical predictions of reverse step flows were made by Roach [20], Taylor and Ndefo [21], and Durst and Pereira [22].

The fission region in the lower corner of the stage was predicted by Alaborn *et al*. [23] after careful study of the sharp expansion of such a channel. Brandt *et al.* [24] and like Bush [25] used the multigrid method, and Lange *et al.* [26] used the method of refinement of local blocks for much more accurate prediction of the result. Armaly *et al.* [16] detailed experimental work with the step geometry having $H/h = 1.94$. Kim and Moin [27] made calculations using the second-order space-time method. Good agreement between theoretical results and experimental values was found for Reynolds numbers up to *500*. The calculated values did not agree with experimental data with Re = *600*. Durst *et al.* [28] further observed the following flow distribution zone in a two-dimensional numerical simulation of a symmetric flow with a sharp expansion. Kaiktsis *et al.* [29] found that the instability was created by convective instability.

The governing equations of fluid and gas mechanics are usually considered to be highly nonlinear, making it difficult to obtain accurate solutions through theoretical analysis. Experimental fluid mechanics plays an important role, but has its limitations [46-48]. In numerical fluid dynamics simulations, many methods require discretization of the computational domain using a grid. Mesh quality and speed have a significant impact on the accuracy and efficiency of numerical simulations.

Many problems of hydro and aerodynamics can have dynamically singular or almost singular solutions in localized flow regions, such as shock waves, boundary layers, detonation waves, etc. In such cases, discretizing the entire region using a uniform mesh may be inefficient because a large number of spatial nodes Capturing the solution in areas of high spatial activity may require the use of very fine grids concentrated in a small portion of the computational domain. Therefore, developing efficient and robust adaptive mesh methods becomes a necessity. Using an ideal adaptive mesh strategy can improve the accuracy of numerical simulations and reduce computational costs. Accordingly, the literature on adaptive moving mesh techniques is growing rapidly, and there are related books and review articles available in scientific publications [30-33, 50].

In this paper, fluid flow with sudden expansion was investigated numerically for 2D - channel with expansion coefficient (H/h) = *2*. Other flow characteristics were calculated at different Reynolds numbers (Re = from *100* to *1000*), to identify and obtain essentially the flow behavior. Calculations are performed for the laminar flow regime. Finally, the studied values such as horizontal velocity, lift-off length, the results were compared with the available experimental values.

The end result of this work is a study of the influence of computational grids on the solution of an internal problem of aerohydromechanics. Thus, along with studying the flow structure after the bench, the goal was to test adaptive and simple meshes for calculating complex flows characterized by the presence of regions with variable flow. To solve the full Navier-Stokes equation, the McCormack scheme was used [34].

2. Physical and mathematical formulation of the problem.

We consider laminar flow in a flat two-dimensional channel with sudden expansion. To understand the position of the fluid through the rear-facing stepped channel, the step length is assumed $h = 5\,mm$. The physical and mathematical formulation of the problem of the analyzed laminar separated flow and the configuration of the computational domain are presented in Fig.1.

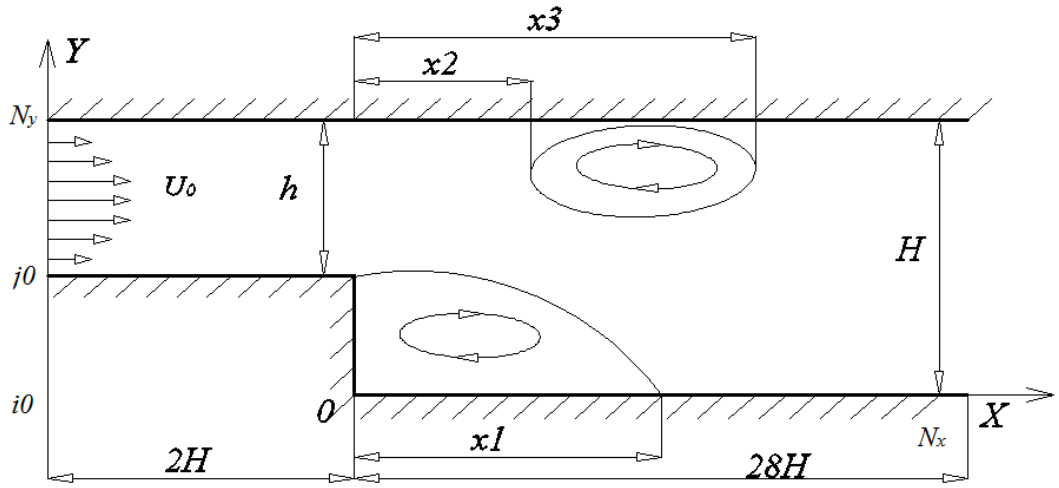

Fig.1. Diagram of the design area in a flat channel with a reverse ledge.

To solve the problem, a Cartesian coordinate system was introduced, the origin of which is located in the lower left corner in front of the protrusions. The width of the smaller channel in the left input part is h, and in the right output part of the channel it doubles and is equal to $H = 2h$. The height of the ledge is also *h*. The channel length is defined as $L = 30H$. At the entrance to the channel, a parabolic Poiseuille flow profile was specified for the longitudinal velocity -*U*, transverse velocity -*V* and pressure -*p*, which is equal to zero. To describe the fluid motion, nonstationary Navier-Stokes equations were used in incompressible form without any simplifying assumptions. For the dimensionless length value, the width of the wider part of the channel was chosen - *H*, and for the dimensionless speed - the average flow rate at the entrance to the channel. The length of the attachment of the primary vortex after the step at the bottom of the channel is denoted as x_1, the length of the secondary vortex formed after the step at the top of the channel is denoted as X_{ab}, the length of the beginning of the secondary vortex is x_2, and the length of the end of the secondary vortex is x_3.

System of dimensionless nonstationary two-dimensional Navier-Stokes equations and continuity equations with constant density $\rho = const$ in Cartesian coordinates has the following form [35]:

$$\begin{cases} \dfrac{\partial U}{\partial t} + U\dfrac{\partial U}{\partial x} + V\dfrac{\partial U}{\partial y} + \dfrac{\partial p}{\rho \partial x} = \dfrac{1}{\mathrm{Re}}\left(\dfrac{\partial^2 U}{\partial y^2} + \dfrac{\partial^2 U}{\partial x^2}\right), \\ \dfrac{\partial V}{\partial t} + U\dfrac{\partial V}{\partial x} + V\dfrac{\partial V}{\partial y} + \dfrac{\partial p}{\rho \partial y} = \dfrac{1}{\mathrm{Re}}\left(\dfrac{\partial^2 V}{\partial y^2} + \dfrac{\partial^2 V}{\partial x^2}\right), \\ \dfrac{\partial U}{\partial x} + \dfrac{\partial V}{\partial y} = 0, \end{cases} \tag{2.1}$$

here U, V - respectively, the dimensionless longitudinal and vertical components of the laminar flow velocity vector, p - dimensionless hydrostatic pressure, $\mathrm{Re} = HU_0 / \nu$ - Reynolds number.

Initial conditions. It is assumed that in all sections of the channel the condition of fully developed flow and longitudinal velocity U has a parabolic Poiseuille profile in the form:

$$\begin{cases} i0 \le x \le 0, \\ j0 \le y \le Ny, \end{cases} \quad U[x,y,0] = \frac{3\left(y\left(1 + \frac{j0}{Ny} \right) - y^2 - \frac{j0}{Ny} \right)}{\left(1 - \frac{j0^3}{Ny} \right)}, \quad V[x,y,0] = 0, \quad p[x,y,0] = 0,$$

$$\begin{cases} x > 0, \\ 0 \le y \le Ny, \end{cases} \quad U[x,y,0] = 3(1-y)y, \quad V[x,y,0] = 0, \quad p[x,y,0] = 0, \tag{2.2}$$

boundary conditions

$$\begin{aligned} & U[Nx,y] = \frac{\partial U}{\partial x}, \quad V[Nx,y] = \frac{\partial V}{\partial x}, \quad p[Nx,y] = \frac{\partial p}{\partial x}, \\ & U[x,Ny] = 0, \quad V[x,Ny] = 0, \quad p[x,Ny] = \frac{\partial p}{\partial y}, \\ & x \le 0 \quad U[x,j0] = 0, \quad V[x,j0] = 0, \quad p[x,j0] = \frac{\partial p}{\partial y}, \\ & x > 0 \quad U[x,0] = 0, \quad V[x,0] = 0, \quad p[x,0] = \frac{\partial p}{\partial y}. \end{aligned} \tag{2.3}$$

3. Navier-Stokes equation in new independent variables

In many non-stationary problems, features of the solution region, such as areas with large gradients, shift and change their position over time. Therefore, it is necessary to use movable grids that adapt to changes in the solution over time. Such meshes that dynamically adapt to the solution are called dynamically adaptive [36-39].

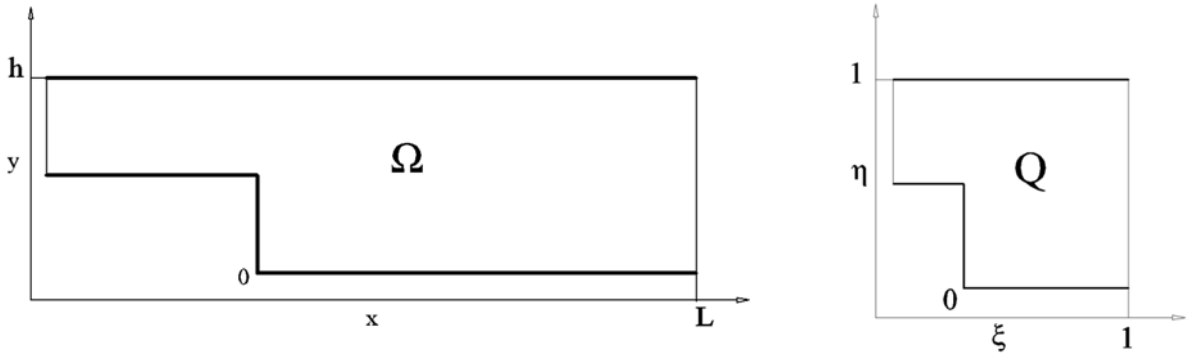

Fig.2. Physical area mapping Ω on the computing domain Q.

In the two-dimensional case, to construct a difference scheme on a moving grid, you must first write the original problem in the computational domain. The construction of moving grids is based on coordinate transformation:

$$x = x(\xi,\eta,t), \quad y = y(\xi,\eta,t) \tag{3.1}$$

which is at every moment of time t establishes a one-to-one continuously differentiable correspondence between the physical domain Ω and the computing domain Q simple form - unit square (see Fig.2).

By virtue of the equalities

$$\Phi\left(x(\xi,\eta,t), y(\xi,\eta,t), t\right) \to \Phi(\xi,\eta,t). \tag{3.2}$$

Then, by the rule of differentiation of complex functions, we obtain that:

$$\begin{cases} \dfrac{\partial \Phi}{\partial t}(x,y,t) = \dfrac{\partial \Phi}{\partial \xi}\dfrac{\partial \xi}{\partial t} + \dfrac{\partial \Phi}{\partial \eta}\dfrac{\partial \eta}{\partial t} + \dfrac{\partial \Phi}{\partial t}\dfrac{\partial t}{\partial t}, \\ \dfrac{\partial \Phi}{\partial x}(x,y,t) = \dfrac{\partial \Phi}{\partial \xi}\dfrac{\partial \xi}{\partial x} + \dfrac{\partial \Phi}{\partial \eta}\dfrac{\partial \eta}{\partial x}, \\ \dfrac{\partial \Phi}{\partial y}(x,y,t) = \dfrac{\partial \Phi}{\partial \xi}\dfrac{\partial \xi}{\partial y} + \dfrac{\partial \Phi}{\partial \eta}\dfrac{\partial \eta}{\partial y}, \end{cases} \tag{3.3}$$

here $\Phi = U, V, p$.

To do this, we differentiate the identity $x = x\left(\xi(x,y,t), \eta(x,y,t), t\right)$, and $y = y\left(\xi(x,y,t), \eta(x,y,t), t\right)$, first by variable x and y, and then - by t:

Let's differentiate the variable by direction x. From the system of equations, we determine $\dfrac{\partial \xi}{\partial x}$ and $\dfrac{\partial \eta}{\partial x}$:

$$\begin{cases} 1 = \dfrac{\partial x}{\partial \xi}\dfrac{\partial \xi}{\partial x} + \dfrac{\partial x}{\partial \eta}\dfrac{\partial \eta}{\partial x}, \\ 0 = \dfrac{\partial y}{\partial \xi}\dfrac{\partial \xi}{\partial x} + \dfrac{\partial y}{\partial \eta}\dfrac{\partial \eta}{\partial x}. \end{cases} \tag{3.4}$$

From here $\dfrac{\partial \xi}{\partial x} = \dfrac{1}{J}\dfrac{\partial y}{\partial \eta}, \quad \dfrac{\partial \eta}{\partial x} = -\dfrac{1}{J}\dfrac{\partial y}{\partial \xi}$. Where $J = \left(\dfrac{\partial y}{\partial \eta}\dfrac{\partial x}{\partial \xi} - \dfrac{\partial y}{\partial \xi}\dfrac{\partial x}{\partial \eta}\right)$ - Jacobian transformation.

Let's differentiate the variable by direction y. From the system of equations, we determine $\dfrac{\partial \xi}{\partial y}$ and $\dfrac{\partial \eta}{\partial y}$:

$$\begin{cases} 0 = \dfrac{\partial x}{\partial \xi}\dfrac{\partial \xi}{\partial y} + \dfrac{\partial x}{\partial \eta}\dfrac{\partial \eta}{\partial y}, \\ 1 = \dfrac{\partial y}{\partial \xi}\dfrac{\partial \xi}{\partial y} + \dfrac{\partial y}{\partial \eta}\dfrac{\partial \eta}{\partial y}, \end{cases} \tag{3.5}$$

from here

$$\frac{\partial \xi}{\partial y} = -\frac{1}{J}\frac{\partial x}{\partial \eta}, \qquad \frac{\partial \eta}{\partial y} = \frac{1}{J}\frac{\partial x}{\partial \xi}.$$

Let's differentiate by time variable *t*. From the system of equations, we determine $\frac{\partial \eta}{\partial t}$:

$$\begin{cases} 0 = \dfrac{\partial x}{\partial \xi}\dfrac{\partial \xi}{\partial t} + \dfrac{\partial x}{\partial \eta}\dfrac{\partial \eta}{\partial t} + \dfrac{\partial x}{\partial t}\dfrac{\partial t}{\partial t}, \\ 0 = \dfrac{\partial y}{\partial \xi}\dfrac{\partial \xi}{\partial t} + \dfrac{\partial y}{\partial \eta}\dfrac{\partial \eta}{\partial t} + \dfrac{\partial y}{\partial t}\dfrac{\partial t}{\partial t}, \end{cases} \tag{3.6}$$

from here $$\frac{\partial \eta}{\partial t} = -\frac{1}{J}\left(\frac{\partial y}{\partial t}\frac{\partial x}{\partial \xi} - \frac{\partial x}{\partial t}\frac{\partial y}{\partial \xi}\right).$$

Let's differentiate by time variable *t*. From the system of equations, we determine $\frac{\partial \xi}{\partial t}$:

from here

$$\frac{\partial \xi}{\partial t} = -\frac{1}{J}\left(\frac{\partial y}{\partial \eta}\frac{\partial x}{\partial t} - \frac{\partial y}{\partial t}\frac{\partial x}{\partial \eta}\right).$$

Hence

$$\begin{cases} \dfrac{\partial \Phi}{\partial t} = \dfrac{\partial \Phi}{\partial t} - \dfrac{1}{J}\dfrac{\partial \Phi}{\partial \xi}\left(\dfrac{\partial y}{\partial \eta}\dfrac{\partial x}{\partial t} - \dfrac{\partial y}{\partial t}\dfrac{\partial x}{\partial \eta}\right) - \dfrac{1}{J}\dfrac{\partial \Phi}{\partial \eta}\left(\dfrac{\partial y}{\partial t}\dfrac{\partial x}{\partial \xi} - \dfrac{\partial x}{\partial t}\dfrac{\partial y}{\partial \xi}\right), \\ \dfrac{\partial \Phi}{\partial x} = \dfrac{1}{J}\dfrac{\partial \Phi}{\partial \xi}\dfrac{\partial y}{\partial \eta} - \dfrac{1}{J}\dfrac{\partial \Phi}{\partial \eta}\dfrac{\partial y}{\partial \xi}, \\ \dfrac{\partial \Phi}{\partial y} = -\dfrac{1}{J}\dfrac{\partial \Phi}{\partial \xi}\dfrac{\partial x}{\partial \eta} + \dfrac{1}{J}\dfrac{\partial \Phi}{\partial \eta}\dfrac{\partial x}{\partial \xi}, \\ \dfrac{\partial^2 \Phi}{\partial x^2} = \dfrac{1}{J}\dfrac{\partial y}{\partial \eta}\dfrac{\partial}{\partial \xi}\left(\dfrac{1}{J}\dfrac{\partial y}{\partial \eta}\dfrac{\partial \Phi}{\partial \xi} - \dfrac{1}{J}\dfrac{\partial y}{\partial \xi}\dfrac{\partial \Phi}{\partial \eta}\right) - \dfrac{1}{J}\dfrac{\partial y}{\partial \xi}\dfrac{\partial}{\partial \eta}\left(\dfrac{1}{J}\dfrac{\partial y}{\partial \eta}\dfrac{\partial \Phi}{\partial \xi} - \dfrac{1}{J}\dfrac{\partial y}{\partial \xi}\dfrac{\partial \Phi}{\partial \eta}\right), \\ \dfrac{\partial^2 \Phi}{\partial y^2} = \dfrac{1}{J}\dfrac{\partial x}{\partial \xi}\dfrac{\partial}{\partial \eta}\left(\dfrac{1}{J}\dfrac{\partial x}{\partial \xi}\dfrac{\partial \Phi}{\partial \eta} - \dfrac{1}{J}\dfrac{\partial x}{\partial \eta}\dfrac{\partial \Phi}{\partial \xi}\right) - \dfrac{1}{J}\dfrac{\partial x}{\partial \eta}\dfrac{\partial}{\partial \xi}\left(\dfrac{1}{J}\dfrac{\partial x}{\partial \xi}\dfrac{\partial \Phi}{\partial \eta} - \dfrac{1}{J}\dfrac{\partial x}{\partial \eta}\dfrac{\partial \Phi}{\partial \xi}\right). \end{cases} \tag{3.7}$$

and Eq.(3.1) is written in new coordinates as the following equation in non-divergent form:

$$
\begin{cases}
\dfrac{\partial U}{\partial t}+U\left(\dfrac{1}{J}\left(\dfrac{\partial y}{\partial \eta}-\dfrac{\partial x}{\partial \eta}-\left(\dfrac{\partial y}{\partial \eta}\dfrac{\partial x}{\partial t}-\dfrac{\partial y}{\partial t}\dfrac{\partial x}{\partial \eta}\right)\right)\right)\dfrac{\partial U}{\partial \xi}+V\left(\dfrac{1}{J}\left(\dfrac{\partial x}{\partial \xi}-\dfrac{\partial y}{\partial \xi}-\left(\dfrac{\partial y}{\partial t}\dfrac{\partial x}{\partial \xi}-\dfrac{\partial x}{\partial t}\dfrac{\partial y}{\partial \xi}\right)\right)\right)\dfrac{\partial U}{\partial \eta}+ \\
+\dfrac{1}{J}\dfrac{\partial y}{\partial \eta}\dfrac{\partial p}{\rho \partial \xi}-\dfrac{1}{J}\dfrac{\partial y}{\partial \xi}\dfrac{\partial p}{\rho \partial \eta}=\dfrac{1}{\mathrm{Re}}\left[\dfrac{1}{J}\dfrac{\partial}{\partial \xi}\left(\left(\dfrac{1}{J}\left(\left(\dfrac{\partial y}{\partial \eta}\right)^2+\left(\dfrac{\partial x}{\partial \eta}\right)^2\right)\right)\dfrac{\partial U}{\partial \xi}\right)+\right. \\
\left.+\left(-\dfrac{1}{J}\dfrac{\partial}{\partial \xi}\left(\left(\dfrac{1}{J}\left(\dfrac{\partial y}{\partial \xi}\dfrac{\partial y}{\partial \eta}+\dfrac{\partial x}{\partial \xi}\dfrac{\partial x}{\partial \eta}\right)\right)\dfrac{\partial U}{\partial \eta}\right)\right)\right]+ \\
+\dfrac{1}{\mathrm{Re}}\left(\dfrac{1}{J}\dfrac{\partial}{\partial \eta}\left(\left(\dfrac{1}{J}\left(\left(\dfrac{\partial y}{\partial \xi}\right)^2+\left(\dfrac{\partial x}{\partial \xi}\right)^2\right)\right)\dfrac{\partial U}{\partial \eta}\right)-\dfrac{1}{J}\dfrac{\partial}{\partial \eta}\left(\left(\dfrac{1}{J}\left(\dfrac{\partial y}{\partial \xi}\dfrac{\partial y}{\partial \eta}+\dfrac{\partial x}{\partial \xi}\dfrac{\partial x}{\partial \eta}\right)\right)\dfrac{\partial U}{\partial \xi}\right)\right), \\
\dfrac{\partial V}{\partial t}+U\left(\dfrac{1}{J}\left(\dfrac{\partial y}{\partial \eta}-\dfrac{\partial x}{\partial \eta}-\left(\dfrac{\partial y}{\partial \eta}\dfrac{\partial x}{\partial t}-\dfrac{\partial y}{\partial t}\dfrac{\partial x}{\partial \eta}\right)\right)\right)\dfrac{\partial V}{\partial \xi}+ \\
+V\left(\dfrac{1}{J}\left(\dfrac{\partial x}{\partial \xi}-\dfrac{\partial y}{\partial \xi}-\left(\dfrac{\partial y}{\partial t}\dfrac{\partial x}{\partial \xi}-\dfrac{\partial x}{\partial t}\dfrac{\partial y}{\partial \xi}\right)\right)\right)\dfrac{\partial V}{\partial \eta}+\dfrac{1}{J}\dfrac{\partial x}{\partial \xi}\dfrac{\partial p}{\rho \partial \eta}-\dfrac{1}{J}\dfrac{\partial x}{\partial \eta}\dfrac{\partial p}{\rho \partial \xi}= \\
=\dfrac{1}{\mathrm{Re}}\left(\dfrac{1}{J}\dfrac{\partial}{\partial \xi}\left(\left(\dfrac{1}{J}\left(\left(\dfrac{\partial y}{\partial \eta}\right)^2+\left(\dfrac{\partial x}{\partial \eta}\right)^2\right)\right)\dfrac{\partial V}{\partial \xi}\right)-\dfrac{1}{J}\dfrac{\partial}{\partial \xi}\left(\left(\dfrac{1}{J}\left(\dfrac{\partial y}{\partial \xi}\dfrac{\partial y}{\partial \eta}+\dfrac{\partial x}{\partial \xi}\dfrac{\partial x}{\partial \eta}\right)\right)\dfrac{\partial V}{\partial \eta}\right)\right)+ \\
+\dfrac{1}{\mathrm{Re}}\left(\dfrac{1}{J}\dfrac{\partial}{\partial \eta}\left(\left(\dfrac{1}{J}\left(\left(\dfrac{\partial y}{\partial \xi}\right)^2+\left(\dfrac{\partial x}{\partial \xi}\right)^2\right)\right)\dfrac{\partial V}{\partial \eta}\right)-\dfrac{1}{J}\dfrac{\partial}{\partial \eta}\left(\left(\dfrac{1}{J}\left(\dfrac{\partial y}{\partial \xi}\dfrac{\partial y}{\partial \eta}+\dfrac{\partial x}{\partial \xi}\dfrac{\partial x}{\partial \eta}\right)\right)\dfrac{\partial V}{\partial \xi}\right)\right), \\
\dfrac{1}{J}\dfrac{\partial y}{\partial \eta}\dfrac{\partial U}{\partial \xi}-\dfrac{1}{J}\dfrac{\partial y}{\partial \xi}\dfrac{\partial U}{\partial \eta}+\dfrac{1}{J}\dfrac{\partial x}{\partial \xi}\dfrac{\partial V}{\partial \eta}-\dfrac{1}{J}\dfrac{\partial x}{\partial \eta}\dfrac{\partial V}{\partial \xi}=0.
\end{cases}
\tag{3.8}
$$

4. Two-dimensional equidistribution method

Let us consider methods for constructing curvilinear grids in which the coordinates of grid nodes are determined by solving partial differential equations [40]. Some methods use parabolic equations, others use hyperbolic ones, but the most widely used are differential methods for constructing grids based on solving elliptic equations.

In non-stationary problems, the adaptive mesh must be rebuilt at each time step, since the solution to the problem depends on time. Let us indicate the method we use to calculate the coordinates of nodes $\mathbf{x}_{i,j}^{n}$ on $(n+1)$ -*m* layer under the assumption that the grid already exists on the *n*-*m* layer in time and the solution is calculated on it $\mathbf{U}_{i,j}^{n}$.

To determine the location of nodes $\mathbf{x}_{i,j}^{n+1}$.You can use the equidistribution method. However, when solving one-dimensional problems, it was discovered [41] that the use of the classical equidistribution method for constructing moving adaptive grids can lead to oscillations of the trajectories of adaptive grid nodes and non-monotonic changes in the ratios of the lengths of neighboring grid cells. In addition, the solution to the classical equation is very sensitive to disturbances in the control function, and the constructed mesh can oscillate strongly in time even when the solution changes slightly. Therefore, in [42] it was recommended to

add the right side to the equation of the classical equidistribution method, which is responsible for the smoothness of the trajectories of grid nodes. We will also use this empirically obtained recommendation in the two-dimensional case: to construct moving meshes we will use a two-dimensional analogue of the one-dimensional evolution equation from [42]:

$$\begin{cases} \dfrac{\partial}{\partial\xi}\left(\omega_1 g_{22}\dfrac{\partial x}{\partial\xi}\right)+\dfrac{\partial}{\partial\eta}\left(\omega_2 g_{11}\dfrac{\partial x}{\partial\eta}\right)=\beta\dfrac{\partial x}{\partial t}, \\ \dfrac{\partial}{\partial\xi}\left(\omega_1 g_{22}\dfrac{\partial y}{\partial\xi}\right)+\dfrac{\partial}{\partial\eta}\left(\omega_2 g_{11}\dfrac{\partial y}{\partial\eta}\right)=\beta\dfrac{\partial y}{\partial t}, \end{cases} \tag{4.1}$$

where

$$g_{11}=\left(\frac{\partial x}{\partial\xi}\right)^2+\left(\frac{\partial y}{\partial\xi}\right)^2,\quad g_{22}=\left(\frac{\partial x}{\partial\eta}\right)^2+\left(\frac{\partial y}{\partial\eta}\right)^2,$$

$$\omega_1=\sqrt{1+\alpha\left(\left|\frac{\partial U}{\partial x}\right|+\left|\frac{\partial V}{\partial x}\right|\right)},\quad \omega_2=\sqrt{1+\alpha\left(\left|\frac{\partial U}{\partial y}\right|+\left|\frac{\partial V}{\partial y}\right|\right)}$$

where ω - control function, β a positive parameter selected experimentally in order to reduce oscillations of the trajectories of grid nodes. When the parameter value is small β member influence β insignificantly, but at large β the displacement values of the nodes decrease and the mesh becomes "sedentary" on the tasks parameter α was equal to *1*.

Boundary conditions $x[Nx,j]=L,\ y[Nx,j]=\dfrac{\partial y}{\partial\xi},\quad x[i,Ny]=\dfrac{\partial x}{\partial\eta},\quad y[i,Ny]=h.$

For the numerical solution of the Navier-Stokes Eq.(3.8), the McCormack scheme was used, and for Eq.(4.1), the variable direction scheme was used.

5. Numerical schemes. MacCormack-MC scheme

In computational fluid dynamics, the McCormack method is a widely used discretization scheme for the numerical solution of hyperbolic partial differential equations [30]. This two-step second-order finite difference method was proposed by Robert and McCormack. This scheme is especially useful for solving nonlinear PDE such as the Euler and Navier-Stokes equations. Let's write the Navier-Stokes Eq.(3.1) in new coordinates in the following matrix form:

$$\begin{aligned} &\frac{\partial\Phi}{\partial t}+\mathrm{A}U\frac{\partial\Phi}{\partial\xi}+\mathrm{B}V\frac{\partial\Phi}{\partial\eta}+\Pi^{\Phi}= \\ &=\frac{1}{\mathrm{Re}}\left(\frac{1}{J}\frac{\partial}{\partial\xi}\left(\mathrm{E}\frac{\partial\Phi}{\partial\xi}\right)-\frac{1}{J}\frac{\partial}{\partial\xi}\left(\Gamma\frac{\partial\Phi}{\partial\eta}\right)\right)+\frac{1}{\mathrm{Re}}\left(\frac{1}{J}\frac{\partial}{\partial\eta}\left(\mathrm{H}\frac{\partial\Phi}{\partial\eta}\right)-\frac{1}{J}\frac{\partial}{\partial\eta}\left(\mathrm{M}\frac{\partial\Phi}{\partial\xi}\right)\right), \end{aligned} \tag{5.1}$$

here

$$\Phi=\begin{pmatrix}U\\V\end{pmatrix},\quad \mathrm{A}=\begin{pmatrix}\frac{1}{J}\left(\frac{\partial y}{\partial\eta}-\frac{\partial x}{\partial\eta}-\left(\frac{\partial y}{\partial\eta}\frac{\partial x}{\partial t}-\frac{\partial y}{\partial t}\frac{\partial x}{\partial\eta}\right)\right)\\ \frac{1}{J}\left(\frac{\partial y}{\partial\eta}-\frac{\partial x}{\partial\eta}-\left(\frac{\partial y}{\partial\eta}\frac{\partial x}{\partial t}-\frac{\partial y}{\partial t}\frac{\partial x}{\partial\eta}\right)\right)\end{pmatrix},\quad \mathrm{B}=\begin{pmatrix}\frac{1}{J}\left(\frac{\partial x}{\partial\xi}-\frac{\partial y}{\partial\xi}-\left(\frac{\partial y}{\partial t}\frac{\partial x}{\partial\xi}-\frac{\partial x}{\partial t}\frac{\partial y}{\partial\xi}\right)\right)\\ \frac{1}{J}\left(\frac{\partial x}{\partial\xi}-\frac{\partial y}{\partial\xi}-\left(\frac{\partial y}{\partial t}\frac{\partial x}{\partial\xi}-\frac{\partial x}{\partial t}\frac{\partial y}{\partial\xi}\right)\right)\end{pmatrix},$$

$$\Pi^{\Phi}=\begin{pmatrix}\frac{1}{J}\frac{\partial y}{\partial\eta}\frac{\partial p}{\rho\partial\xi}-\frac{1}{J}\frac{\partial y}{\partial\xi}\frac{\partial p}{\rho\partial\eta}\\ \frac{1}{J}\frac{\partial x}{\partial\xi}\frac{\partial p}{\rho\partial\eta}-\frac{1}{J}\frac{\partial x}{\partial\eta}\frac{\partial p}{\rho\partial\xi}\end{pmatrix},\quad \mathrm{E}=\begin{pmatrix}\frac{1}{J}\left(\left(\frac{\partial y}{\partial\eta}\right)^2+\left(\frac{\partial x}{\partial\eta}\right)^2\right)\\ \frac{1}{J}\left(\left(\frac{\partial y}{\partial\eta}\right)^2+\left(\frac{\partial x}{\partial\eta}\right)^2\right)\end{pmatrix},\quad \Gamma=\begin{pmatrix}\frac{1}{J}\left(\frac{\partial y}{\partial\xi}\frac{\partial y}{\partial\eta}+\frac{\partial x}{\partial\xi}\frac{\partial x}{\partial\eta}\right)\\ \frac{1}{J}\left(\frac{\partial y}{\partial\xi}\frac{\partial y}{\partial\eta}+\frac{\partial x}{\partial\xi}\frac{\partial x}{\partial\eta}\right)\end{pmatrix},$$

$$\mathrm{H}=\begin{pmatrix}\frac{1}{J}\left(\left(\frac{\partial y}{\partial\xi}\right)^2+\left(\frac{\partial x}{\partial\xi}\right)^2\right)\\ \frac{1}{J}\left(\left(\frac{\partial y}{\partial\xi}\right)^2+\left(\frac{\partial x}{\partial\xi}\right)^2\right)\end{pmatrix},\quad \mathrm{M}=\begin{pmatrix}\frac{1}{J}\left(\frac{\partial y}{\partial\xi}\frac{\partial y}{\partial\eta}+\frac{\partial x}{\partial\xi}\frac{\partial x}{\partial\eta}\right)\\ \frac{1}{J}\left(\frac{\partial y}{\partial\xi}\frac{\partial y}{\partial\eta}+\frac{\partial x}{\partial\xi}\frac{\partial x}{\partial\eta}\right)\end{pmatrix}.$$

Applying the explicit two-step predictor-corrector method to the nonlinear Navier-Stokes equation, the following difference scheme is obtained:

Predictor

$$\begin{aligned}\bar{\Phi}_{i,j}&=\Phi^n_{i,j}-\Delta t\left(\mathrm{A}U^n_{i,j}\frac{\Phi^n_{i+1,j}-\Phi^n_{i,j}}{\Delta\xi}+\mathrm{B}V^n_{i,j}\frac{\Phi^n_{i,j+1}-\Phi^n_{i,j}}{\Delta\eta}\right)+\\
&+\Delta t\frac{1}{J\,\mathrm{Re}}\left\{\frac{\left(\mathrm{E}_{i,j}+\mathrm{E}_{i+1,j}\right)}{2\Delta\xi^2}\Phi^n_{i+1,j}-\frac{\left(\mathrm{E}_{i-1,j}+2\mathrm{E}_{i,j}+\mathrm{E}_{i+1,j}\right)}{2\Delta\xi^2}\Phi^n_{i,j}+\right.\\
&\left.+\frac{\left(\mathrm{E}_{i,j}+\mathrm{E}_{i-1,j}\right)}{2\Delta\xi^2}\Phi^n_{i-1,j}\right\}+\Delta t\frac{1}{J\,\mathrm{Re}}\frac{1}{2\Delta\xi}\left\{\Gamma_{i+1,j}\frac{\Phi^n_{i+1,j+1}-\Phi^n_{i+1,j-1}}{2\Delta\eta}-\right.\\
&\left.+\Gamma_{i-1,j}\frac{\Phi^n_{i-1,j+1}-\Phi^n_{i-1,j-1}}{2\Delta\eta}\right\}+\Delta t\frac{1}{J\,\mathrm{Re}}\left\{\frac{\left(\mathrm{H}_{i,j}+\mathrm{H}_{i,j+1}\right)}{2\Delta\eta^2}\Phi^n_{i,j+1}-\right.\\
&\left.+\frac{\left(\mathrm{H}_{i,j-1}+2\mathrm{H}_{i,j}+\mathrm{H}_{i,j+1}\right)}{2\Delta\eta^2}\Phi^n_{i,j}+\frac{\left(\mathrm{H}_{i,j}+\mathrm{H}_{i,j-1}\right)}{2\Delta\eta^2}\Phi^n_{i,j-1}\right\}+\\
&+\Delta t\frac{1}{J\,\mathrm{Re}}\frac{1}{2\Delta\eta}\left(\mathrm{M}_{i,j+1}\frac{\Phi^n_{i+1,j+1}-\Phi^n_{i-1,j+1}}{2\Delta\xi}-\mathrm{M}_{i,j+1}\frac{\Phi^n_{i+1,j-1}-\Phi^n_{i-1,j-1}}{2\Delta\xi}\right).\end{aligned}\tag{5.2}$$

Corrector

$$\Phi_{i,j}^{n+1}=\frac{1}{2}\left\{\bar{\Phi}_{i,j}+\Phi_{i,j}^{n}-\Delta t\left(\mathrm{A}\bar{U}_{i,j}^{n}\frac{\bar{\Phi}_{i,j}^{n}-\bar{\Phi}_{i-1,j}^{n}}{\Delta\xi}+\mathrm{B}\bar{V}_{i,j}^{n}\frac{\bar{\Phi}_{i,j}^{n}-\bar{\Phi}_{i,j-1}^{n}}{\Delta\eta}\right)+\right.$$
$$+\Delta t\frac{1}{J\,\mathrm{Re}}\left(\frac{\left(\mathrm{E}_{i,j}+\mathrm{E}_{i+1,j}\right)}{2\Delta\xi^{2}}\bar{\Phi}_{i+1,j}^{n}-\frac{\left(\mathrm{E}_{i-1,j}+2\mathrm{E}_{i,j}+\mathrm{E}_{i+1,j}\right)}{2\Delta\xi^{2}}\bar{\Phi}_{i,j}^{n}+\frac{\left(\mathrm{E}_{i,j}+\mathrm{E}_{i-1,j}\right)}{2\Delta\xi^{2}}\bar{\Phi}_{i-1,j}^{n}\right)+$$
$$+\Delta t\frac{1}{J\,\mathrm{Re}}\frac{1}{2\Delta\xi}\left(\Gamma_{i+1,j}\frac{\bar{\Phi}_{i+1,j+1}^{n}-\bar{\Phi}_{i+1,j-1}^{n}}{2\Delta\eta}-\Gamma_{i-1,j}\frac{\bar{\Phi}_{i-1,j+1}^{n}-\bar{\Phi}_{i-1,j-1}^{n}}{2\Delta\eta}\right)+ \tag{5.3}$$
$$+\Delta t\frac{1}{J\,\mathrm{Re}}\left(\frac{\left(\mathrm{H}_{i,j}+\mathrm{H}_{i,j+1}\right)}{2\Delta\eta^{2}}\bar{\Phi}_{i,j+1}^{n}-\frac{\left(\mathrm{H}_{i,j-1}+2\mathrm{H}_{i,j}+\mathrm{H}_{i,j+1}\right)}{2\Delta\eta^{2}}\bar{\Phi}_{i,j}^{n}+\frac{\left(\mathrm{H}_{i,j}+\mathrm{H}_{i,j-1}\right)}{2\Delta\eta^{2}}\bar{\Phi}_{i,j-1}^{n}\right)+$$
$$\left.+\Delta t\frac{1}{J\,\mathrm{Re}}\frac{1}{2\Delta\eta}\left(\Gamma_{i,j+1}\frac{\bar{\Phi}_{i+1,j+1}^{n}-\bar{\Phi}_{i-1,j+1}^{n}}{2\Delta\xi}-\Gamma_{i,j+1}\frac{\bar{\Phi}_{i+1,j-1}^{n}-\bar{\Phi}_{i-1,j-1}^{n}}{2\Delta\xi}\right)\right\}.$$

This is an explicit scheme of second order accuracy in time and space with an approximation error $O\left((\Delta t)^{2},(\Delta x)^{2},(\Delta y)^{2}\right)$.

Initially (predictor) the estimate is found $\overline{\Phi_{i}^{n+1}}$ values and at the $n+1$ -*m* time step, and then (corrector) the final value is determined Φ_{i}^{n+1} on $n+1$ -*m* time step. Please note that in the predictor it is approximated by direct differences, and in the corrector by inverse differences.

The method of variable directions was used for the numerical solution of Eq.(4.1). Let 's replace the differential problem with a difference analog of the following form:

$$\begin{cases}\beta\dfrac{\mathbf{x}_{i,j}^{n+1/2}-\mathbf{x}_{i,j}^{n}}{0.5\Delta t}=\dfrac{1}{\Delta\xi}\left(\omega_{i+1/2,j}g_{22,i+1/2,j}\dfrac{\mathbf{x}_{i+1,j}^{n+1/2}-\mathbf{x}_{i,j}^{n+1/2}}{\Delta\xi}-\omega_{i-1/2,j}g_{22,i-1/2,j}\dfrac{\mathbf{x}_{i,j}^{n+1/2}-\mathbf{x}_{i-1,j}^{n+1/2}}{\Delta\xi}\right)+\\ +\dfrac{1}{\Delta\eta}\left(\omega_{i,j+1/2}g_{11,i,j+1/2}\dfrac{\mathbf{x}_{i,j+1}^{n}-\mathbf{x}_{i,j}^{n}}{\Delta\eta}-\omega_{i,j-1/2}g_{11,i,j-1/2}\dfrac{\mathbf{x}_{i,j}^{n}-\mathbf{x}_{i,j-1}^{n}}{\Delta\eta}\right),\\ \beta\dfrac{\mathbf{x}_{i,j}^{n+1}-\mathbf{x}_{i,j}^{n+1/2}}{0.5\Delta t}=\dfrac{1}{\Delta\xi}\left(\omega_{i+1/2,j}g_{22,i+1/2,j}\dfrac{\mathbf{x}_{i+1,j}^{n+1/2}-\mathbf{x}_{i,j}^{n+1/2}}{\Delta\xi}-\omega_{i-1/2,j}g_{22,i-1/2,j}\dfrac{\mathbf{x}_{i,j}^{n+1/2}-\mathbf{x}_{i-1,j}^{n+1/2}}{\Delta\xi}\right)+\\ +\dfrac{1}{\Delta\eta}\left(\omega_{i,j+1/2}g_{11,i,j+1/2}\dfrac{\mathbf{x}_{i,j+1}^{n+1}-\mathbf{x}_{i,j}^{n+1}}{\Delta\eta}-\omega_{i,j-1/2}g_{11,i,j-1/2}\dfrac{\mathbf{x}_{i,j}^{n+1}-\mathbf{x}_{i,j-1}^{n+1}}{\Delta\eta}\right).\end{cases} \tag{5.4}$$

Here n - number of iterative approximation, τ - iteration parameter, since the components of the metric tensor depend on the solution, the coefficients g_{11}, g_{22} calculated using the solution n - st iteration. The velocity obtained according to the schemes Eq.(5.3) does not satisfy the continuity Eq.(5.4). Therefore, we make a correction to the SIMPLE procedure [43]. $\delta p_{i,j}$, which satisfies the condition of non-uniformity, in the new coordinate has the following form:

$$\begin{cases} \tilde{U}^{n+1} = U^{n+1} + \Delta t\left(\frac{1}{J}\frac{\partial U^{n+1}}{\partial \xi}\left(\frac{\partial y}{\partial \eta}\frac{\partial x}{\partial t} - \frac{\partial y}{\partial t}\frac{\partial x}{\partial \eta}\right) + \frac{1}{J}\frac{\partial U^{n+1}}{\partial \eta}\left(\frac{\partial y}{\partial t}\frac{\partial x}{\partial \xi} - \frac{\partial x}{\partial t}\frac{\partial y}{\partial \xi}\right)\right) - \\ +\Delta t\left(\frac{1}{J}\frac{\partial \delta p}{\partial \xi}\frac{\partial y}{\partial \eta} - \frac{1}{J}\frac{\partial \delta p}{\partial \eta}\frac{\partial y}{\partial \xi}\right), \\ \tilde{V}^{n+1} = V^{n+1} + \Delta t\left(\frac{1}{J}\frac{\partial V^{n+1}}{\partial \xi}\left(\frac{\partial y}{\partial \eta}\frac{\partial x}{\partial t} - \frac{\partial y}{\partial t}\frac{\partial x}{\partial \eta}\right) + \frac{1}{J}\frac{\partial V^{n+1}}{\partial \eta}\left(\frac{\partial y}{\partial t}\frac{\partial x}{\partial \xi} - \frac{\partial x}{\partial t}\frac{\partial y}{\partial \xi}\right)\right) - \\ +\Delta t\left(-\frac{1}{J}\frac{\partial p}{\partial \xi}\frac{\partial x}{\partial \eta} + \frac{1}{J}\frac{\partial p}{\partial \eta}\frac{\partial x}{\partial \xi}\right). \end{cases} \tag{5.5}$$

Substituting the velocity now $\tilde{U}_{i,j}^{n+1}, \tilde{V}_{i,j}^{n+1}$ in the continuity equation it is easy to obtain a parabolic equation for the pressure correction in the new coordinate has the following form:

$$\begin{cases} \frac{\partial \delta p}{\partial t} - \frac{1}{J}\left(\frac{\partial y}{\partial \eta}\frac{\partial x}{\partial t} - \frac{\partial y}{\partial t}\frac{\partial x}{\partial \eta}\right)\frac{\partial \delta p}{\partial \xi} - \frac{1}{J}\left(\frac{\partial y}{\partial t}\frac{\partial x}{\partial \xi} - \frac{\partial x}{\partial t}\frac{\partial y}{\partial \xi}\right)\frac{\partial \delta p}{\partial \eta} - \\ +\frac{1}{J}\frac{\partial}{\partial \xi}\left(\left(\frac{1}{J}\left(\left(\frac{\partial y}{\partial \eta}\right)^2 + \left(\frac{\partial x}{\partial \eta}\right)^2\right)\right)\frac{\partial \delta p}{\partial \xi}\right) - \frac{1}{J}\frac{\partial}{\partial \eta}\left(\left(\frac{1}{J}\left(\left(\frac{\partial y}{\partial \xi}\right)^2 + \left(\frac{\partial x}{\partial \xi}\right)^2\right)\right)\frac{\partial \delta p}{\partial \eta}\right) + \\ +\frac{1}{J}\frac{\partial}{\partial \xi}\left(\left(\frac{1}{J}\left(\frac{\partial y}{\partial \xi}\frac{\partial y}{\partial \eta} + \frac{\partial x}{\partial \xi}\frac{\partial x}{\partial \eta}\right)\right)\frac{\partial \delta p}{\partial \eta}\right) + \frac{1}{J}\frac{\partial}{\partial \eta}\left(\left(\frac{1}{J}\left(\frac{\partial y}{\partial \xi}\frac{\partial y}{\partial \eta} + \frac{\partial x}{\partial \xi}\frac{\partial x}{\partial \eta}\right)\right)\frac{\partial \delta p}{\partial \xi}\right) = \\ = -\frac{1}{\Delta t}\left(\frac{1}{J}\frac{\partial y}{\partial \eta}\frac{\partial U}{\partial \xi} - \frac{1}{J}\frac{\partial y}{\partial \xi}\frac{\partial U}{\partial \eta} - \frac{1}{J}\frac{\partial x}{\partial \eta}\frac{\partial V}{\partial \xi} + \frac{1}{J}\frac{\partial x}{\partial \xi}\frac{\partial V}{\partial \eta}\right); \end{cases} \tag{5.6}$$

Let us write Eq.(5.6) in the following form:

$$\begin{aligned} &\frac{\partial \delta p}{\partial t} - \mathrm{A}\frac{\partial \delta p}{\partial \xi} - \mathrm{B}\frac{\partial \delta p}{\partial \eta} - \frac{1}{J}\frac{\partial}{\partial \xi}\left(\mathrm{C}\frac{\partial \delta p}{\partial \xi}\right) - \\ &+\frac{1}{J}\frac{\partial}{\partial \eta}\left(\mathrm{D}\frac{\partial \delta p}{\partial \eta}\right) + \frac{1}{J}\frac{\partial}{\partial \xi}\left(\mathrm{E}\frac{\partial \delta p}{\partial \eta}\right) + \frac{1}{J}\frac{\partial}{\partial \eta}\left(\mathrm{F}\frac{\partial \delta p}{\partial \xi}\right) = \mathrm{G}; \end{aligned} \tag{5.7}$$

here

$$\mathrm{A} = \frac{1}{J}\left(\frac{\partial y}{\partial \eta}\frac{\partial x}{\partial t} - \frac{\partial y}{\partial t}\frac{\partial x}{\partial \eta}\right), \quad \mathrm{B} = \frac{1}{J}\left(\frac{\partial y}{\partial t}\frac{\partial x}{\partial \xi} - \frac{\partial x}{\partial t}\frac{\partial y}{\partial \xi}\right), \quad \mathrm{C} = \left(\frac{1}{J}\left(\left(\frac{\partial y}{\partial \eta}\right)^2 + \left(\frac{\partial x}{\partial \eta}\right)^2\right)\right),$$

$$\mathrm{D} = \left(\frac{1}{J}\left(\left(\frac{\partial y}{\partial \xi}\right)^2 + \left(\frac{\partial x}{\partial \xi}\right)^2\right)\right), \quad \mathrm{E} = \left(\frac{1}{J}\left(\frac{\partial y}{\partial \xi}\frac{\partial y}{\partial \eta} + \frac{\partial x}{\partial \xi}\frac{\partial x}{\partial \eta}\right)\right), \quad \mathrm{F} = \left(\frac{1}{J}\left(\frac{\partial y}{\partial \xi}\frac{\partial y}{\partial \eta} + \frac{\partial x}{\partial \xi}\frac{\partial x}{\partial \eta}\right)\right),$$

$$\mathrm{G} = -\frac{1}{\Delta t}\left(\frac{1}{J}\frac{\partial y}{\partial \eta}\frac{\partial U}{\partial \xi} - \frac{1}{J}\frac{\partial y}{\partial \xi}\frac{\partial U}{\partial \eta} - \frac{1}{J}\frac{\partial x}{\partial \eta}\frac{\partial V}{\partial \xi} + \frac{1}{J}\frac{\partial x}{\partial \xi}\frac{\partial V}{\partial \eta}\right).$$

The method of variable directions was also used for the numerical solution of Eq.(5.7):

$$\begin{cases} \dfrac{\delta p_{i,j}^{n+1/2}-\delta p_{i,j}^{n}}{0.5\Delta t_0}-\mathrm{A}\dfrac{\left(\delta p_{i+1,j}^{n+1/2}-\delta p_{i-1,j}^{n+1/2}\right)}{2\Delta\xi}-\dfrac{1}{J\Delta\xi}\left(\mathrm{C}_{i+1/2,j}\dfrac{\delta p_{i+1,j}^{n+1/2}-\delta p_{i,j}^{n+1/2}}{\Delta\xi}+\mathrm{C}_{i-1/2,j}\times\right. \\ \left.\times\dfrac{\delta p_{i,j}^{n+1/2}-\delta p_{i-1,j}^{n+1/2}}{\Delta\xi}\right)-\mathrm{B}\dfrac{\left(\delta p_{i,j+1}^{n}-\delta p_{i,j-1}^{n}\right)}{2\Delta\eta}-\dfrac{1}{J\Delta\eta}\left(\mathrm{D}_{i,j+1/2}\dfrac{\delta p_{i,j+1}^{n}-\delta p_{i,j}^{n}}{\Delta\eta}-\mathrm{D}_{i,j-1/2}\times\right. \\ \left.\times\dfrac{\delta p_{i,j}^{n}-\delta p_{i,j-1}^{n}}{\Delta\eta}\right)+\dfrac{1}{2\Delta\xi J}\left(\mathrm{E}_{i+1,j}\dfrac{\delta p_{i+1,j+1}^{n}-\delta p_{i+1,j-1}^{n}}{2\Delta\eta}-\mathrm{E}_{i-1,j}\dfrac{\delta p_{i-1,j+1}^{n}-\delta p_{i-1,j-1}^{n}}{2\Delta\eta}\right)+ \\ +\dfrac{1}{2\Delta\eta J}\left(\mathrm{F}_{i,j+1}\dfrac{\delta p_{i+1,j+1}^{n}-\delta p_{i-1,j+1}^{n}}{2\Delta\xi}-\mathrm{F}_{i,j-1}\dfrac{\delta p_{i+1,j-1}^{n}-\delta p_{i-1,j-1}^{n}}{2\Delta\xi}\right)=\mathrm{G} \end{cases} \tag{5.8}$$

$$\begin{cases} \dfrac{\delta p_{i,j}^{n+1}-\delta p_{i,j}^{n+1/2}}{0.5\Delta t_0}-\mathrm{A}\dfrac{\left(\delta p_{i+1,j}^{n+1/2}-\delta p_{i-1,j}^{n+1/2}\right)}{2\Delta\xi}-\dfrac{1}{J\Delta\xi}\left(\mathrm{C}_{i+1/2,j}\dfrac{\delta p_{i+1,j}^{n+1/2}-\delta p_{i,j}^{n+1/2}}{\Delta\xi}-\right. \\ \left.+\mathrm{C}_{i-1/2,j}\dfrac{\delta p_{i,j}^{n+1/2}-\delta p_{i-1,j}^{n+1/2}}{\Delta\xi}\right)-\mathrm{B}\dfrac{\left(\delta p_{i,j+1}^{n+1}-\delta p_{i,j-1}^{n+1}\right)}{2\Delta\eta}- \\ +\dfrac{1}{J\Delta\eta}\left(\mathrm{D}_{i,j+1/2}\dfrac{\delta p_{i,j+1}^{n+1}-\delta p_{i,j}^{n+1}}{\Delta\eta}-\mathrm{D}_{i,j-1/2}\dfrac{\delta p_{i,j}^{n+1}-\delta p_{i,j-1}^{n+1}}{\Delta\eta}\right)+ \\ +\dfrac{1}{2\Delta\xi J}\left(\mathrm{E}_{i+1,j}\dfrac{\delta p_{i+1,j+1}^{n}-\delta p_{i+1,j-1}^{n}}{2\Delta\eta}-\mathrm{E}_{i-1,j}\dfrac{\delta p_{i-1,j+1}^{n}-\delta p_{i-1,j-1}^{n}}{2\Delta\eta}\right)+ \\ +\dfrac{1}{2\Delta\eta J}\left(\mathrm{F}_{i,j+1}\dfrac{\delta p_{i+1,j+1}^{n}-\delta p_{i-1,j+1}^{n}}{2\Delta\xi}-\mathrm{F}_{i,j-1}\dfrac{\delta p_{i+1,j-1}^{n}-\delta p_{i-1,j-1}^{n}}{2\Delta\xi}\right)=\mathrm{G}. \end{cases} \tag{cont. (5.8)}$$

The solution to this problem is as follows:

1) In Eq.(5.4) the initial coordinates are determined.
2) According to Eq.(5.3), intermediate values of the parameters are determined.
3) Then the correction pressure is determined using Eq.(5.8).
4) Consequently, the pressure on the temporary layer $n+1$ will be equal $p^{n+1}=p^{n}+\delta p$.
5) The iterative process continues until the specified accuracy, that is, until the following condition is met: $\max\limits_{1\le i\le n}\left|\tilde{U}_{i,j}^{n+1}-U_{i,j}^{n+1}\right|\le\varepsilon$.

Solution the problem, a rectangular calculation grid 200×100 with the size was used $\Delta x=5/100$, $\Delta y=1/100$, $\Delta t<1/1000$ and the adaptive mesh also used a computational mesh 200×100.

6. Discussion and results

Figure 3 shows the experimental and numerical results of Armali *et al*. for the longitudinal velocity profile, as well as for the two-fluid model for the Reynolds number $\mathrm{Re}=400$. Numerical results for the

McCormack scheme for both a simple mesh and an adaptive mesh. Up to $\mathrm{Re} < 500$, experimental and numerical results did not reveal any additional detachment regions other than the main one attached to the wall. Under these conditions, good agreement between experiments and numerical results is achieved.

This phenomenon is explained by the fact that at such values of the Reynolds number the flow is still laminar and the Navier-Stokes equations are essentially solved. At higher Reynolds numbers, the flow acquires anisotropic turbulence due to recirculation. This explains the discrepancies between the experimental and numerical results shown in Fig.4 at Reynolds number $\mathrm{Re} = 1000$. In these pictures U - dimensionless longitudinal velocity.

Figure 3 shows the results of the longitudinal velocity using different schemes in sections after the ledge. Reynolds number $\mathrm{Re} = 400$. From Fig.3 it can be seen that at low Reynolds numbers, all results give approximately the same result. From Fig.4 it is clear that when using adaptive grids, the parameter describes the parameter very well $(U + x / h)$ by $x / h < 16$ for $\mathrm{Re} = 1000$. Small deviations from experimental data are observed in the range $12 < x / h < 16$.

In Fig.5 shows the results of the length of the primary vortex with a change in the Reynolds number. As we can see from Fig.5, the results of the primary vortex length obtained from different meshes, at $\mathrm{Re} < 400$ are quite close to each other, but the result obtained from different meshes is sharply different when $\mathrm{Re} > 400$. As can be seen in Fig 5, at $\mathrm{Re} > 400$ the result obtained in a simple mesh decreases and the error increases. The results obtained with an adaptive mesh gives a better result. Table 1 shows the design errors for the primary vortex length.

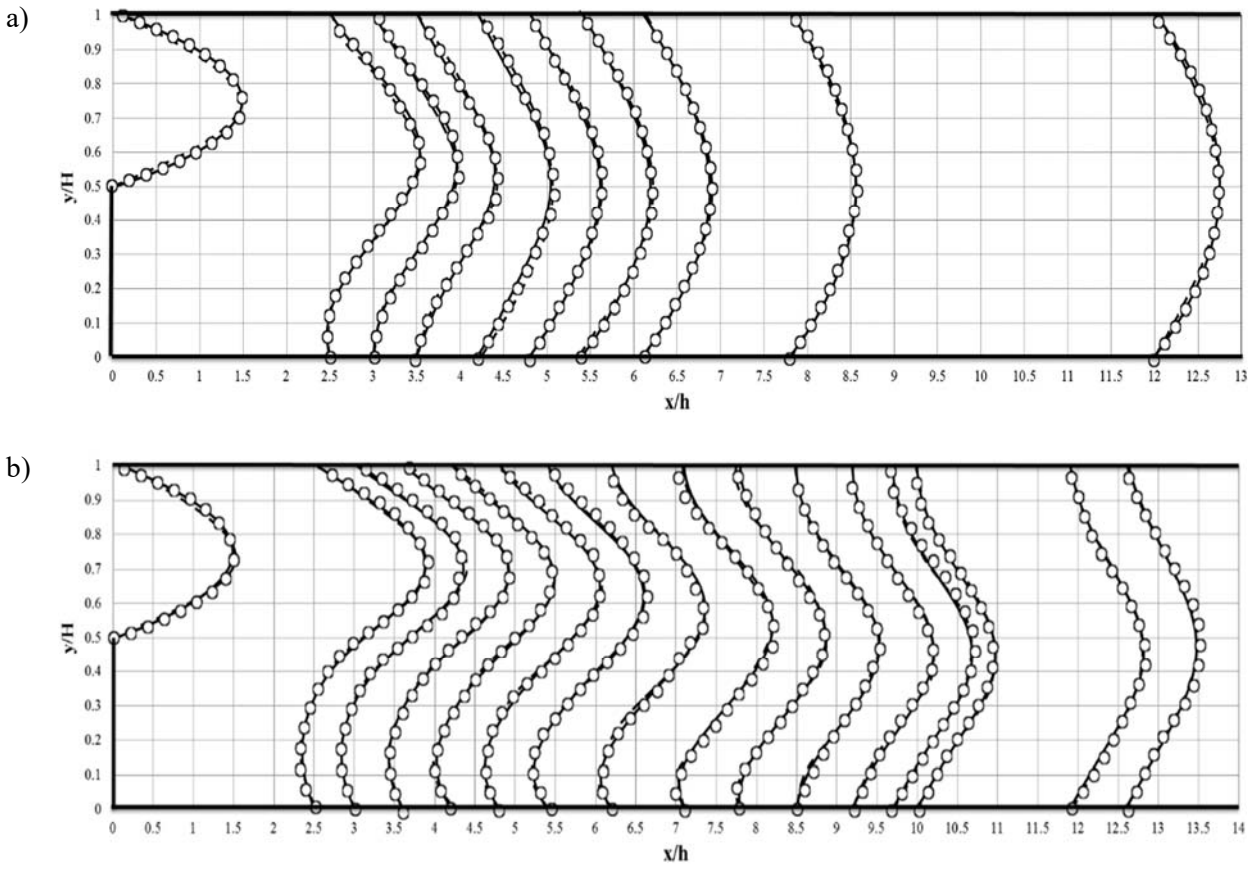

Fig.3. Profiles of the axial $(U + x / h)$ velocity components: (○) Armali *et al.* (experiment), (- - -) McCormack scheme of a simple grid, (---) McCormack's scheme of an adaptive grid.

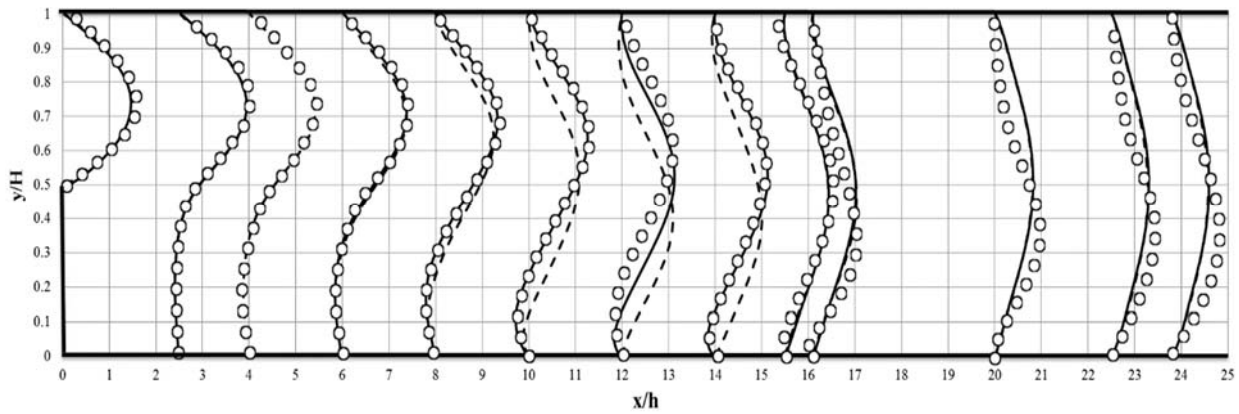

Fig.4. Profiles of the axial $(U + x/h)$velocity components: (○) Armali *et al*. (experiment), (- - -) McCormack scheme of a simple grid, (---) McCormack's scheme of an adaptive grid.

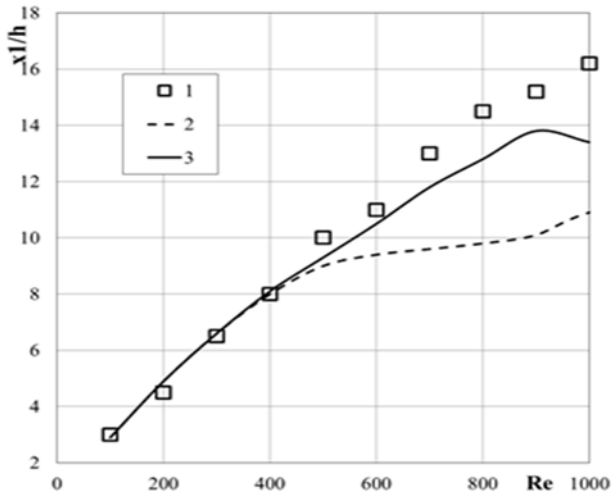

Fig.5. Results the length of the primary vortex with a change in the Reynolds number. (□) Armali *et al*. (experiment), (- - -) McCormack scheme of a simple grid, (---) McCormack scheme of adaptive grid.

Table 1. Scheme errors for primary vortex length.

Number Re	Experiment	Simple mesh	Error %	Adaptive grid	Error %
100	*3*	*2.9*	*3.33*	*2.9*	*3.333*
200	*4.5*	*4.9*	*8.88*	*4.9*	*8.88*
300	*6.5*	*6.6*	*1.538*	*6.6*	*1.53*
400	*8*	*8*	*0*	*8.1*	*1.25*
500	*10*	*9*	*10*	*9.3*	*7*
600	*11*	*9.4*	*14.54*	*10.5*	*4.54*
700	*13*	*9.6*	*26.15*	*11.8*	*9.230*
800	*14.5*	*9.8*	*32.41*	*12.8*	*11.72*
900	*15.2*	*10.1*	*33.55*	*13.8*	*9.210*
1000	*16.2*	*10.9*	*32.71*	*13.4*	*17.28*

Figure 6 shows the results of the length of the secondary vortex with a change in the Reynolds number.

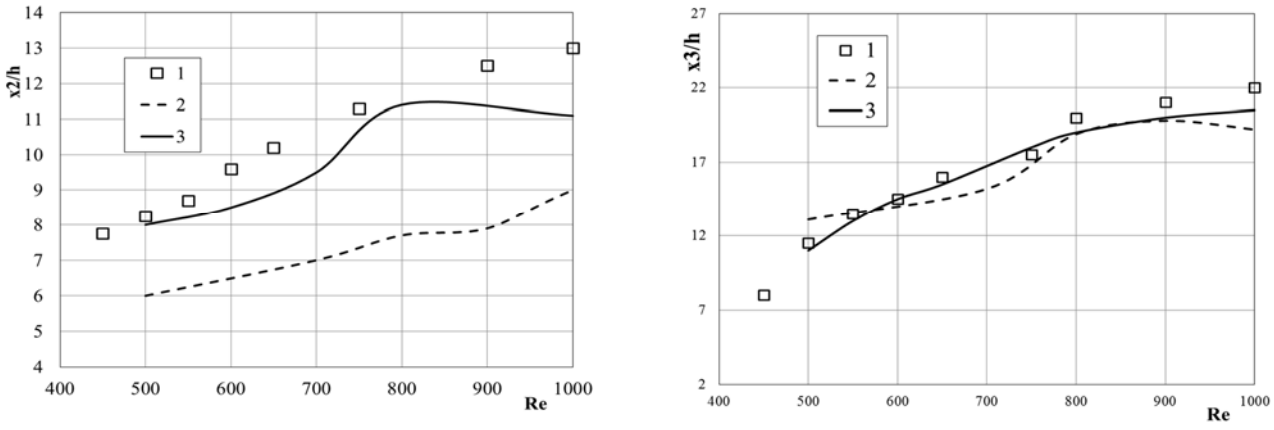

Fig.6. Results of the length of the secondary vortex with a change in the Reynolds number.

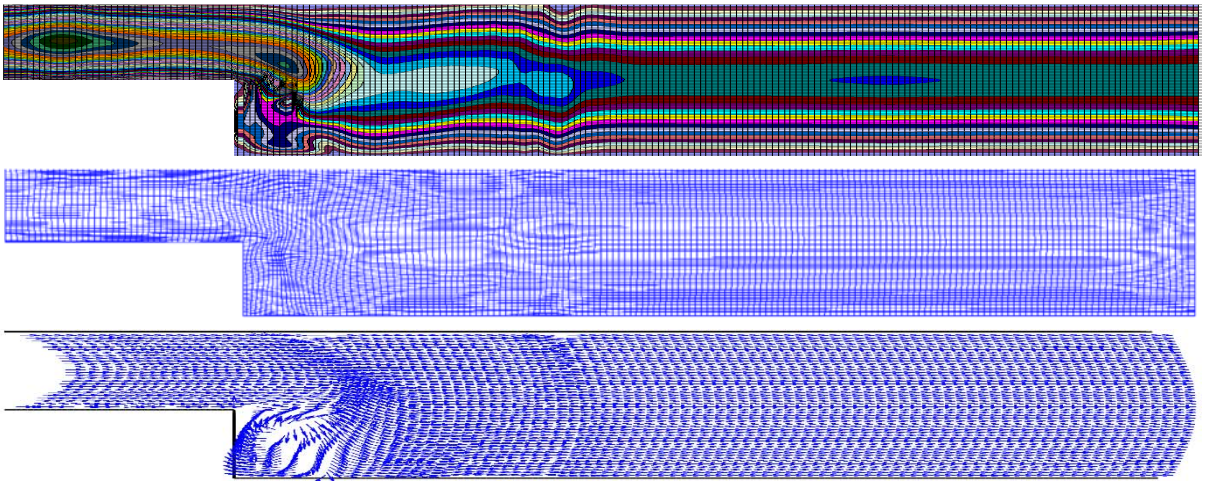

Fig.7a. Changing the adaptive grid, velocity field vector and velocity contour at *T=1*.

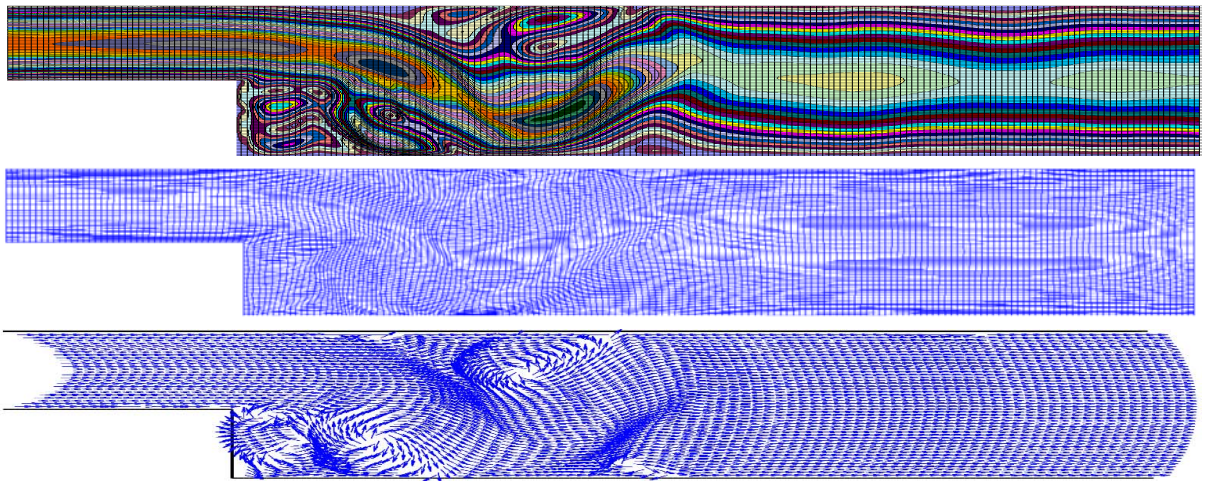

Fig.7b. Changing the adaptive grid, velocity field vector and velocity contour at *T=5*.

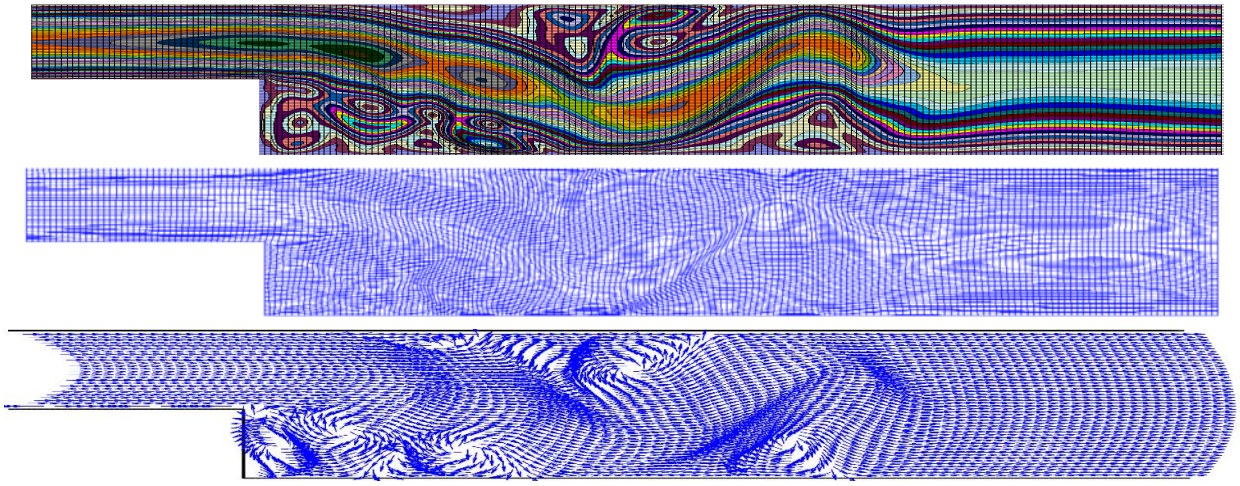

Fig.7c. Changing the adaptive grid, velocity field vector and velocity contour at *T=7.*

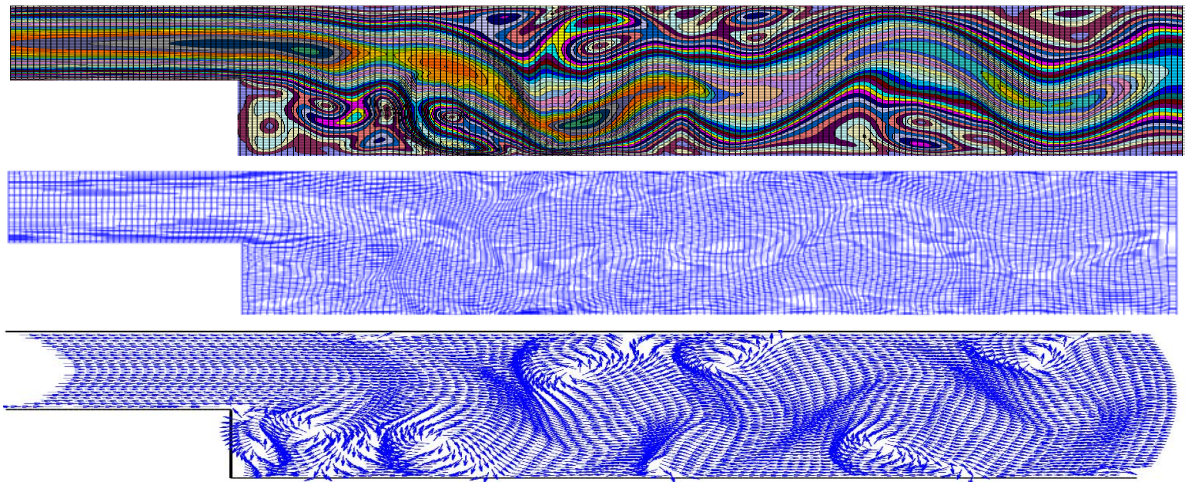

Fig.7d. Changing the adaptive grid, velocity field vector and velocity contour at *T=10.*

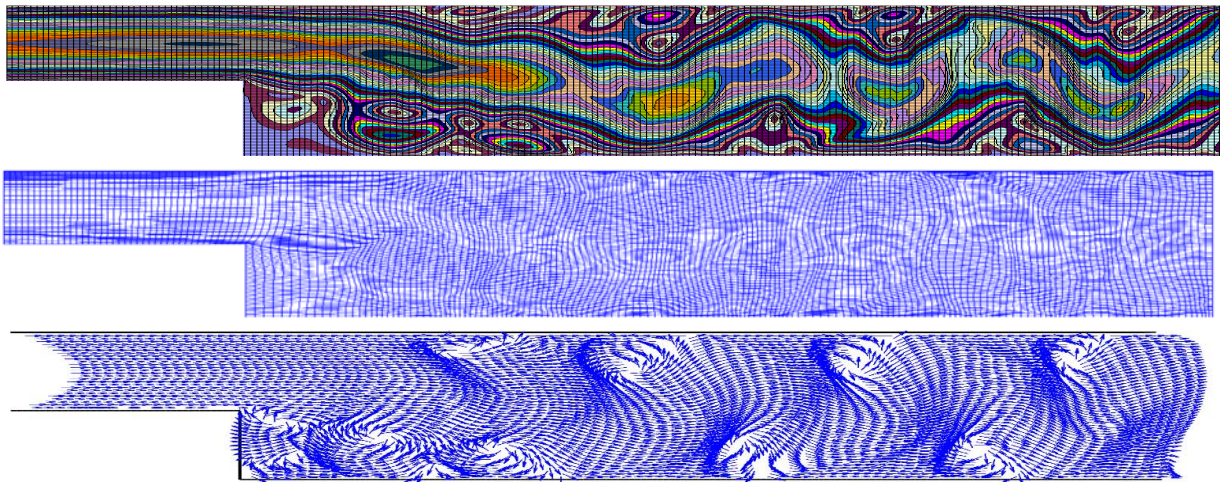

Fig.7e. Changing the adaptive grid, velocity field vector and velocity contour at *T=20.*

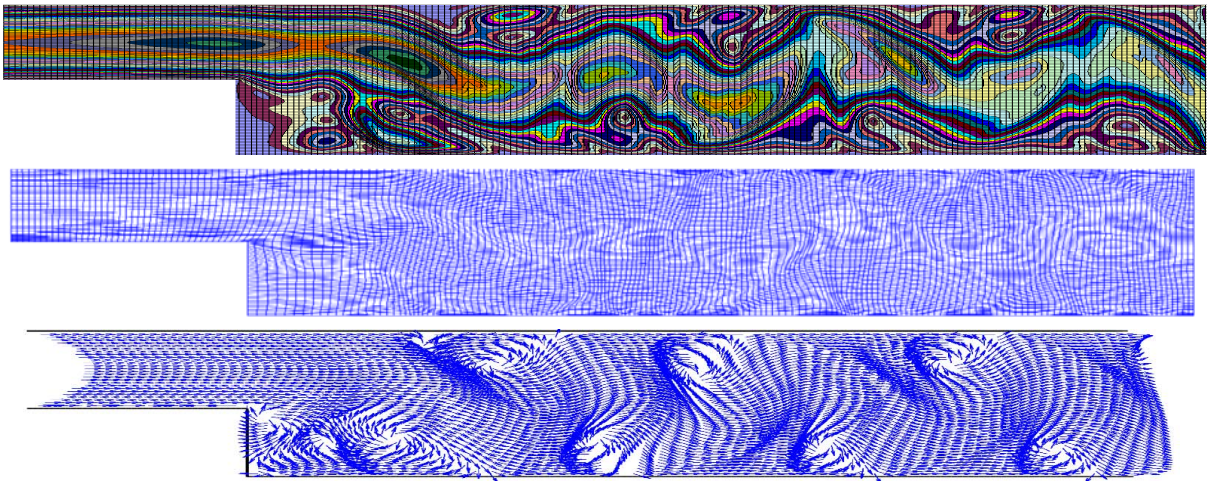

Fig.7f. Changing the adaptive grid, velocity field vector and velocity contour at *T=30.*

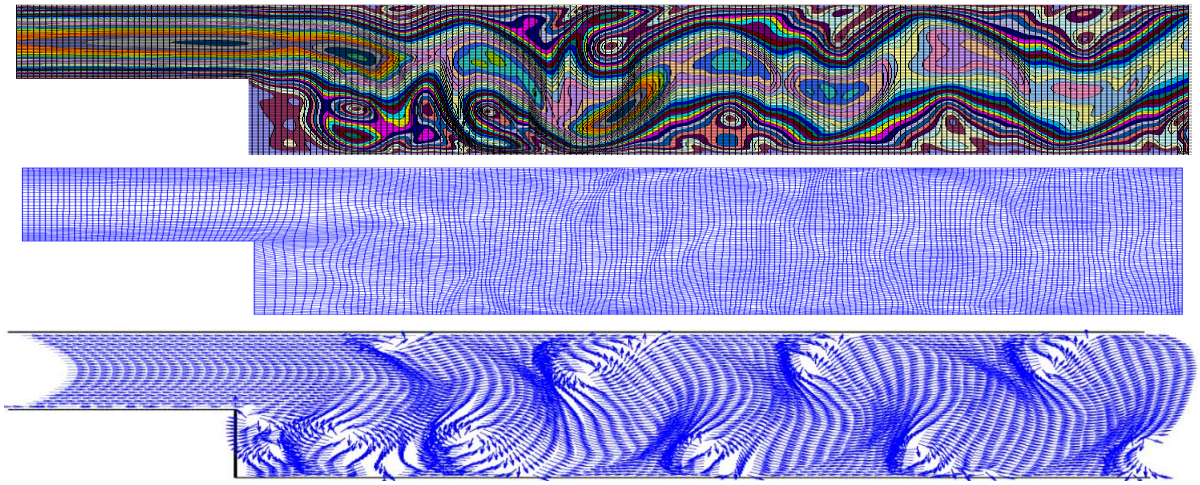

Fig.7g. Changing the adaptive grid, velocity field vector and velocity contour at *T=40.*

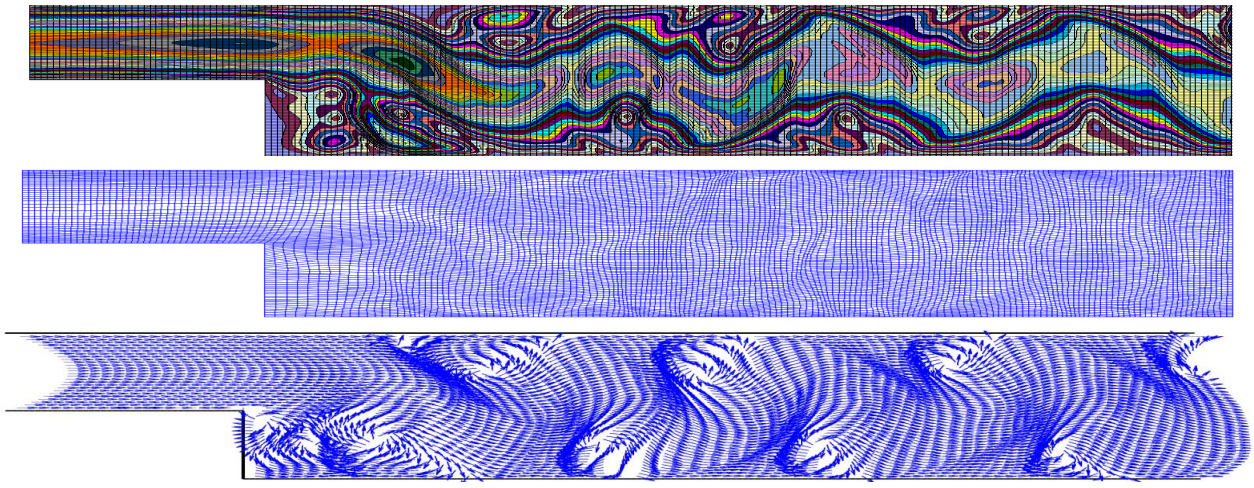

Fig.7h. Changing the adaptive grid, velocity field vector and velocity contour at *T=50.*

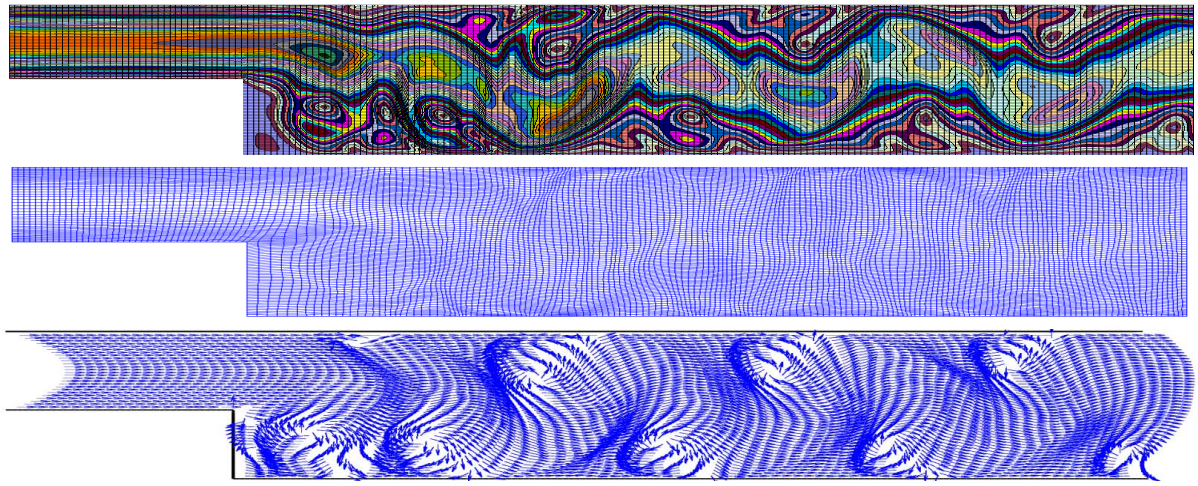

Fig.7i. Changing the adaptive grid, velocity field vector and velocity contour at *T=60.*

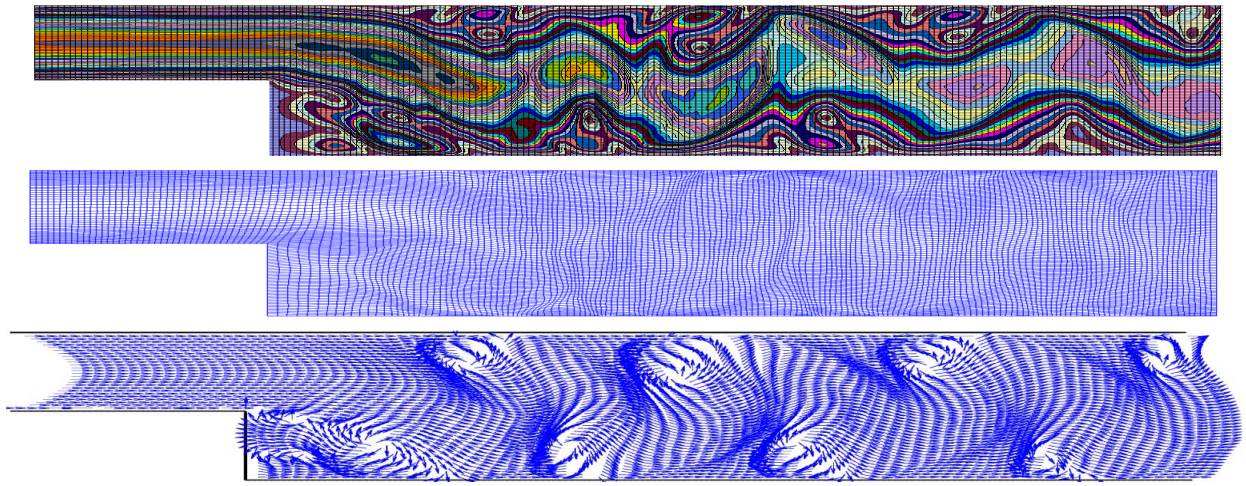

Fig.7j. Changing the adaptive grid, velocity field vector and velocity contour at *T=70.*

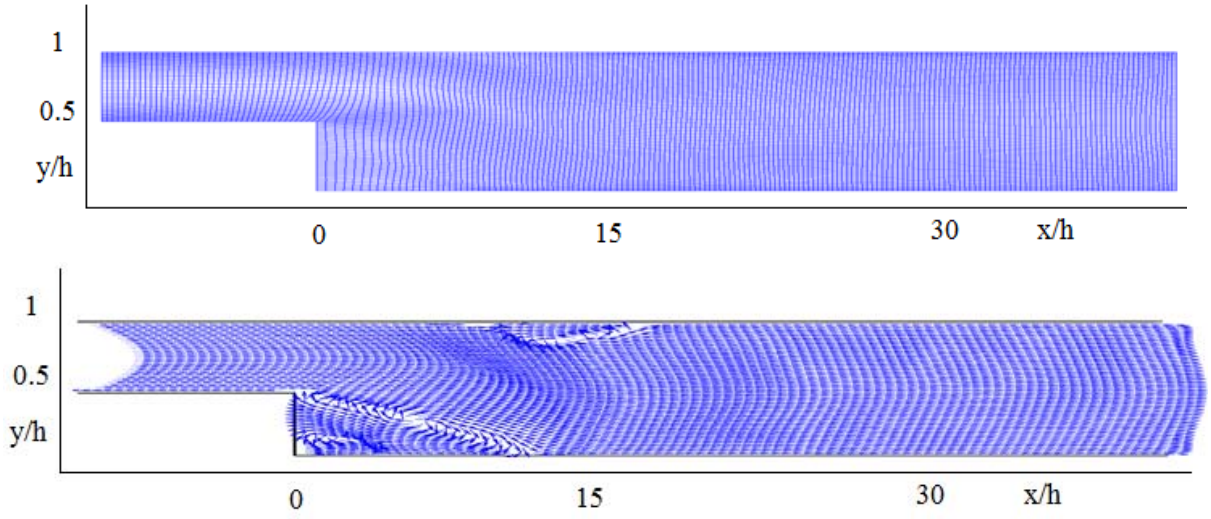

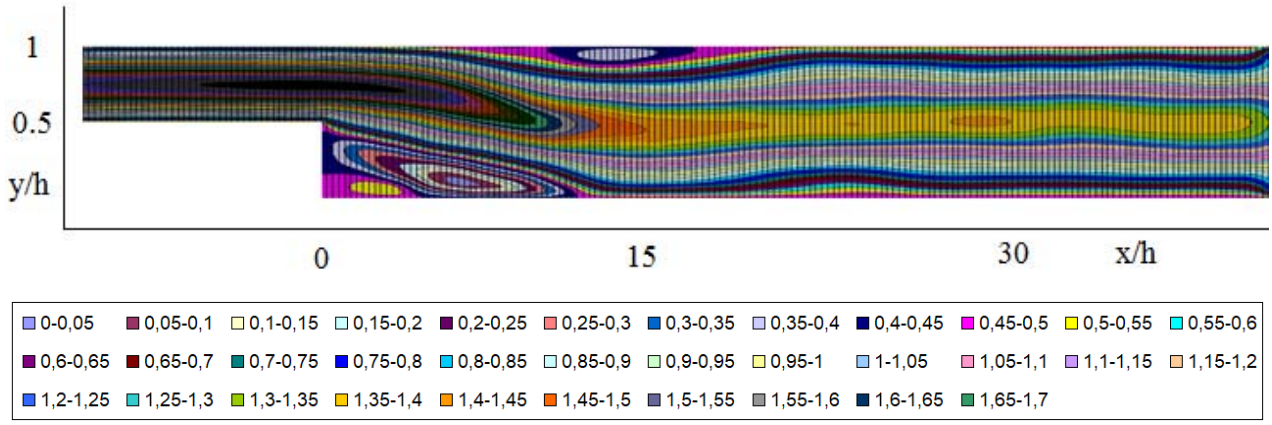

Fig.7k. Change of adaptive grid, velocity field vector and velocity isoline of dimensionless time-averaged velocity.

Figures 7a-7y shows isolines of longitudinal velocity at different times at Reynolds number *Re=1000*.

From the above figures it can be seen that in all cases the zone behind the protrusion is characterized by the formation of reverse flows, and the extent of this zone and the structure of the circulation flow depend not only on the Reynolds number, but also on the computational grid. Numerical studies have shown that the McCormack scheme of second order accuracy, when using adaptive accuracy grids, gives closer results than simple grids [44, 45].

7. Conclusions

This work is a study of methods for adapting the computational grid to solving two-dimensional Navier-Stokes differential equations that describe the physical processes of gas dynamics specifically for the problem of a two-dimensional channel with an expansion coefficient $(H / h) = 2$. The equidistribution method was used to construct a dynamic adaptive grid. Special attention is paid to improving the accuracy of the solution obtained on an adaptive grid. Based on theoretical research, algorithms for solving the Navier-Stokes equations on an adaptive grid in two-dimensional formulations were developed.

The operation of the modules has been tested on 2D problems of gas dynamics that have experimental solutions. For all the considered cases, the solutions obtained on the adaptive mesh well resolved the gas-dynamic features of the problems and were stable. The calculation results confirmed that the use of a dynamic adaptive grid instead of a fixed one leads to a significant reduction in the root-mean-square error of the solution and a reduction in the time required for calculations. This is proof of the effectiveness and efficiency of the proposed algorithms.

The study examined the effect of the McCormack finite difference scheme using the SIMPLE procedure on separation processes. As a result of a detailed numerical analysis of flow velocity fields, patterns of formation of a vortex structure in a flat channel with steps were revealed. This includes secondary vortex formations and unsteady separated flow regimes.

Acknowledgements

The authors of the manuscript gratefully acknowledge the reviewers for their positive feedback and their relevant and constructive comments on our manuscript.

Nomenclature

p – hydrostatic pressure
PDE – partial differential equations
Re – Reynolds number
$\boldsymbol{U}$ – longitudinal components of the velocity vector
$\boldsymbol{V}$ – vertical components of the velocity vector
ω – control function
β – positive parameter

References

[1] Blasius H. (1910): *Laminare stromung in kanalen wechselnder breite*.– Zeitschrift fur Math. und Phys., vol.58, No.10, pp.225-233.

[2] Honji H (1975): *The starting flow down a step*.– *J. Fluid Mech*., vol.69, No.2, pp.229-240. DOI: https://doi.org/10.1017/S0022112075001413

[3] Sinha S.P., Gupta A.K. and Oberai M.M. (1981): *Laminar separation flow around benches and caverns. Part 1. Flow behind the ledge*.– Rocketry and Cosmonautics, vol.19, No.12, pp.33-37.

[4] Armaly B.F., Durst F., Pereira J.C.F. and Schonung B. (1983): *Experimental and theoretical investigation of backward-facing step flow*.– J. Fluid Mech., vol.127, pp.473-496, DOI: https://doi.org/10.1017/S0022112083002839

[5] Zheng P. (1972): *Separated Flows*.– Mir, p.354.

[6] Gogish L.V. and Stepanov G.Yu. (1982): *Turbulent separation flows*.– Fluid Dynamics, vol.17, pp.188-202.

[7] Le H., Moin P. and Kim J. (1997): *Direct numerical simulation of turbulent flow over a backward-facing step*.– J. Fluid Mech., vol.330, pp.349-374, DOI: https://doi.org/10.1017/S0022112096003941.

[8] Durst F., Melling A. and Whitelow J.H. (1974): *Low Reynolds number flow over a plane symmetric sudden expansion*.– J. Fluid Mech., vol.64, No.1, pp.111-118, DOI: https://doi.org/10.1017/S0022112074002035.

[9] Cherdron W., Durst F. and Whitelow J.H. (1978): *Asymmetric flows and instabilities in symmetric ducts with sudden expansions*.– J. Fluid Mech., vol.84, No.1, pp.13-31, DOI: https://doi.org/10.1017/S0022112078000026.

[10] Macadno E.O., and Hung T.-K. (1967): *Computational and experimental study of a captive annular eddy*.– J. Fluid Mech., vol.28, No.1, pp.43-64, DOI: https://doi.org/10.1017/S0022112067001892.

[11] Kumar A. and Yajnik K.S. (1980): *Internal separated flows at large Reynolds number*.– J. Fluid Mech., vol.97, No.1, pp.27-51, DOI: https://doi.org/10.1017/S0022112080002418.

[12] Plotkin A. (1983): *Spectral method calculations of some separated laminar flows in channels*.– Aerospace technology, No.7, pp.75-85.

[13] Acrivos A. and Schrader M.L. (1982): *Steady flow in a sudden expansion at high Reynolds numbers*.– Phys. Fluids, vol.25, No.6, pp.923-930, DOI: https://doi.org/10.1063/1.863844.

[14] Kuon O., Pletcher R. and Lewis J. (1984): *Calculation of sudden expansion flows using boundary layer equations*.– Theor. Fundamentals of Engineering Calculations, vol.106, No.3, pp.116-123.

[15] Lewis J.P. and Pletcher R.H. (1986): *Limits of applicability of boundary layer equations for calculating laminar flows with symmetric sudden expansion*.– Theor. Fundamentals of Engineering Calculation, No.2, pp.284-294.

[16] Malikov Z.M. and Madaliev M.E. (2021): *Numerical simulation of flow in a flat suddenly expanding channel based on a new two-fluid turbulence model*.– Bulletin of MSTU im. N.E. Bauman. Ser. Natural Sciences, vol.97, No.4, pp.24-39, DOI: https://doi.org/10.18698/1812-3368-2021-4-24-39.

[17] Malikov Z.M. and Madaliev M.E. (2022): *Numerical simulation of turbulent flows based on modern turbulence models*.– Computational Mathematics and Mathematical Physics, vol.62, No.10, pp.1707-1722.

[18] Mirzoev A.A. Madaliev M., Sultanbayevich D.Y. and Habibullo ugli A.U. (2020): *Numerical modeling of non-stationary turbulent flow with double barrier based on two liquid turbulence model*.– 2020 International Conference on Information Science and Communications Technologies (ICISCT), IEEE, pp.1-7.

[19] Lee Y.S. and Smith L.C. (1986): *Analysis of Power-Law Viscous Materials Using Complex Stream, Potential and Stress Functions*.– in Encyclopedia of Fluid Mechanics, vol.1, Flow Phenomena and Measurement, ed. N.P. Cheremisinoff, pp.1105-1154.

[20] Roache P.J. (1972): *Computational Fluid Dynamics*.– Hermosa, New Mexico, pp.139-173.

[21] Taylor T.D. and Ndefo E. (1971): *Computation of viscous flow in a channel by the method of splitting*.– Proc. of the Second Int. Conf. on Num. Methods in Fluid Dynamics, Lecture Notes in Physics, vol.8, pp.356-364, Springer Verlag, New York.

[22] Durst F. and Peireira J.C.F. (1988): *Time-dependent laminar backward facing step flow in a two-dimensional duct*.– ASME J. Fluids Eng., vol.110, pp.289-296.

[23] Alleborn N., Nandakumar K., Raszillier H. and Durst F. (1997): *Further contributions on the two-dimensional flow in a sudden expansion*.– J. Fluid Mech., vol.330, pp.169-188.

[24] Brandt A., Dendy J.E. and Ruppel H. (1980): *The multigrid method for semi-implicit hydrodynamic codes*.– *J*. Comput. Phys., vol.34, pp.348-370.

[25] Hackbusch W. (1985): *Multigrid Methods for Applications*.– Springer, Berlin.

[26] Lange C.F., Schäfer M. and Durst F. (2002): *Local block refinement with a multigrid flow solver*.– Int. J. Numer. Methods Fluids, vol.38, pp.21-41.

[27] Kim J. and Moin P. (1985): *Application of a fractional-step method to incompressible Navier-Stokes equations*.– J. Comput. Phys., vol.59, pp.308-323.

[28] Durst F., Peireira J.C.F. and Tropea C. (1993): *The plane symmetric sudden-expansion flow at low Reynolds numbers*.– J. Fluid Mech., vol.248, pp.567-581.

[29] Kaiktsis L., Karniadakis G.E. and Orszag S.A. (1996): *Unsteadiness and convective instabilities in a two-dimensional flow over a backward-facing step*.– J. Fluid Mech., vol.321, pp.157-187.

[30] Baines M.J. (1994): *Moving finite elements*.– Clarendon Press Oxford.

[31] Huang W. and Russell R.D. (2010): *Adaptive Moving Mesh Methods*.– vol.174, Springer Science & Business Media.

[32] Hawken D.F., Gottlieb J.J. and Hansen J.S. (1991): *Review of some adaptive node-movement techniques in finite-element and finite-difference solutions of partial differential equations*.– Journal of Computational Physics, vol.95, No.2, pp.254-302.

[33] Tang T. (2005): *Moving mesh methods for computational fluid dynamics*.– Contemporary Mathematics, vol.383, No.8, pp.141-173, DOI:10.1090/conm/383/07162.

[34] MacCormack R.W. (1969): *The Effect of Viscosity in Hypervelocity Impact Cratering*.– AIAA Paper, pp.69-354, Cincinnati, Ohio, https://doi.org/10.1007/BFb0021338.

[35] Loytsyansky L.G. (1987): *Mechanics of liquid and gas*.– Maskva. Science, pp.678.

[36] Sommer A.F.and Shokina N.Yu. (2012): *On some problems of designing difference schemes on two-dimensional moving grids*.– Computational Technologies, vol.17, No.4, pp.88-108.

[37] Khakimzyanov G.S. and Shokina N.Yu. (1998): *Equidistribution method for constructing adaptive grids*.– Computational technologies. vol.3, No.6. pp.63-81.

[38] Shyy W. (1986): *An adaptive grid method for Navier-Stokes flow computation II: Grid addition*.– Applied numerical mathematics, vol.2, No.1, pp.9-19.

[39] Shyy W., Tong S.S. and Correa S.M. (1985): *Numerical recirculating flow calculation using a body-fitted coordinate system*.– Numerical Heat Transfer. vol.8, No.1, pp.99-113.

[40] Basile F., Chapelier J.-B., de La Llave Plata M., Laraufie R. and Frey P. (2021): *A high-order h-adaptive discontinuous Galerkin method for unstructured grids based on a posteriori error estimation*.– AIAA Scitech 2021 Forum, p.1696.

[41] Huang W. and Zhan X. (2005): *Adaptive moving mesh modeling for two-dimensional groundwater flow and transport*.– Contemporary Mathematics, vol.383, pp.239-252.

[42] Ou K., Liang C. and Jameson A. (2010): *High-order spectral difference method for the Navier-Stokes equation on unstructured moving deformable grid*.– 48th AIAA Aerospace Sciences Meeting Including the New Horizons Forum and Aerospace Exposition, p.541.

[43] Patankar S.V. (1980): *Numerical Heat Transfer and Fluid Flow*.– Taylor & Francis, ISBN 978-0-89116-522-4.

[44] Erkinjon Son M.M. (2021): *Numerical calculation of an air centrifugal separator based on the SARC turbulence model*.– J. Appl. Comput. Mech., vol.6, pp.1133-1140, https://doi.org/10.22055/JACM.2020.31423.1871.

[45] Madaliev E., Madaliev M., Adilov K. and Pulatov T. (2021) *Comparison of turbulence models for two-phase flow in a centrifugal separator*.– in E3S Web of Conferences, vol.264, p.1009, https://doi.org/10.1051/e3sconf/202126401009

[46] Volk B.L., Lagoudas D.C., Chen Y.C. and Whitley K.S. (2010): *Analysis of the finite deformation response of shape memory polymers: I. Thermomechanical characterization*.– Smart Materials and Structures, vol.19, No.7, p.10, DOI: 10.1088/0964-1726/19/7/075005

[47] Ratajczak M., Ptak M., Chybowski L., Gawdzińska K. and Będziński R. (2019): *Material and structural modeling aspects of brain tissue deformation under dynamic loads*.– Materials, MDPI, vol.12, No.2, Article number 271, p.13, doi: 10.3390/ma120271.

[48] Reparaz J.S., Pereira da Silva K., Romero A.H., Serrano J., Wagner M.R., Callsen G., Choi S.J., Speck J.S. and Goñi A.R. (2018): *Comparative study of the pressure dependence of optical-phonon transverse-effective charges and linewidths in wurtzite*.– In N. Phys., Rev.B, vol.98, Article number 165204, DOI: https://doi.org/10.1103/PhysRevB.98.165204.

[49] Kholboev B.M., Navruzov D.P., Asrakulova D.S., Engalicheva N.R. and Turemuratova A.A. (2022): *Comparison of the results for calculation of vortex currents after sudden expansion of the pipe with different diameters*.– Int. J. of Applied Mechanics and Engineering, vol.27, No.2, pp.115-123. https://doi.org/10.2478/ijame-2022-0023.

Received: April 29, 2024
Revised: June 5, 2024